EVALUATION OF DRAG FORCES IN STEEP, ROUGH FLUMES

by

Ashraf Ibrahim Al-Khatib

Thesis submitted to the Graduate Faculty of the

Virginia Polytechnic Institute

in candidacy for the degree of

MASTER OF SCIENCE

in

Civil Engineering

December 1962

Blacksburg, Virginia

TABLE OF CONTENTS

LIST OF FIGURES

LIST OF TABLES

I. INTRODUCTION

Dissipation of kinetic energy contained in water flowing in steep chutes has been a constant menace whenever such dissipation becomes necessary.

Hydraulic investigators have been at variance regarding the choice of the most efficient method to dissipate such energy. Naturally their common aim is to find an efficient mean for such dissipation.

Many methods have been used for this purpose, the most common of which is the induction and control of a hydraulic jump. Here the momentum of fast moving water is balanced by the piezometric head of more tranquil water of greater depth but at lower energy state. Other methods are to induce some type of turbulence or to dissipate the energy by impact against a traverse wall. Another common hydraulic device is a sloping chute with a stilling basin at the end. The dissipation of this errosive energy at once and at one place usually requires a large and expensive stilling basin.

Recent experiments by Mohanty (11) and Al-Khafaji (1) provide the basis for a promising simple and inexpensive method of energy dissipation throughout the entire length of a chute channel by installing properly designed traverse roughness elements. In these experiments the kinetic energy is dissipated due to mainly the effective form drag force offered by each roughness element along the channel.

The importance of the evaluation of drag forces was first fully realized by Al-Khafaji (1). He conducted series of experiments and measured drag forces in all flow regimes existing in his steep channel. From these measured, or rather computed, drag forces he developed an equation expressing the drag force, offered by each two-dimensional roughness element, in terms of measurable quantities. Such evaluation was made only for tumbling regime, however.

The purpose of this thesis is to evaluate the drag forces in rapid and tranquil regimes. It is further hoped to find a correlation between the drag coefficient, C_D, and Chezy coefficient, C, in the rapid regime.

This thesis is based on data collected by Al-Khafaji at the hydraulic laboratories at Utah State University.

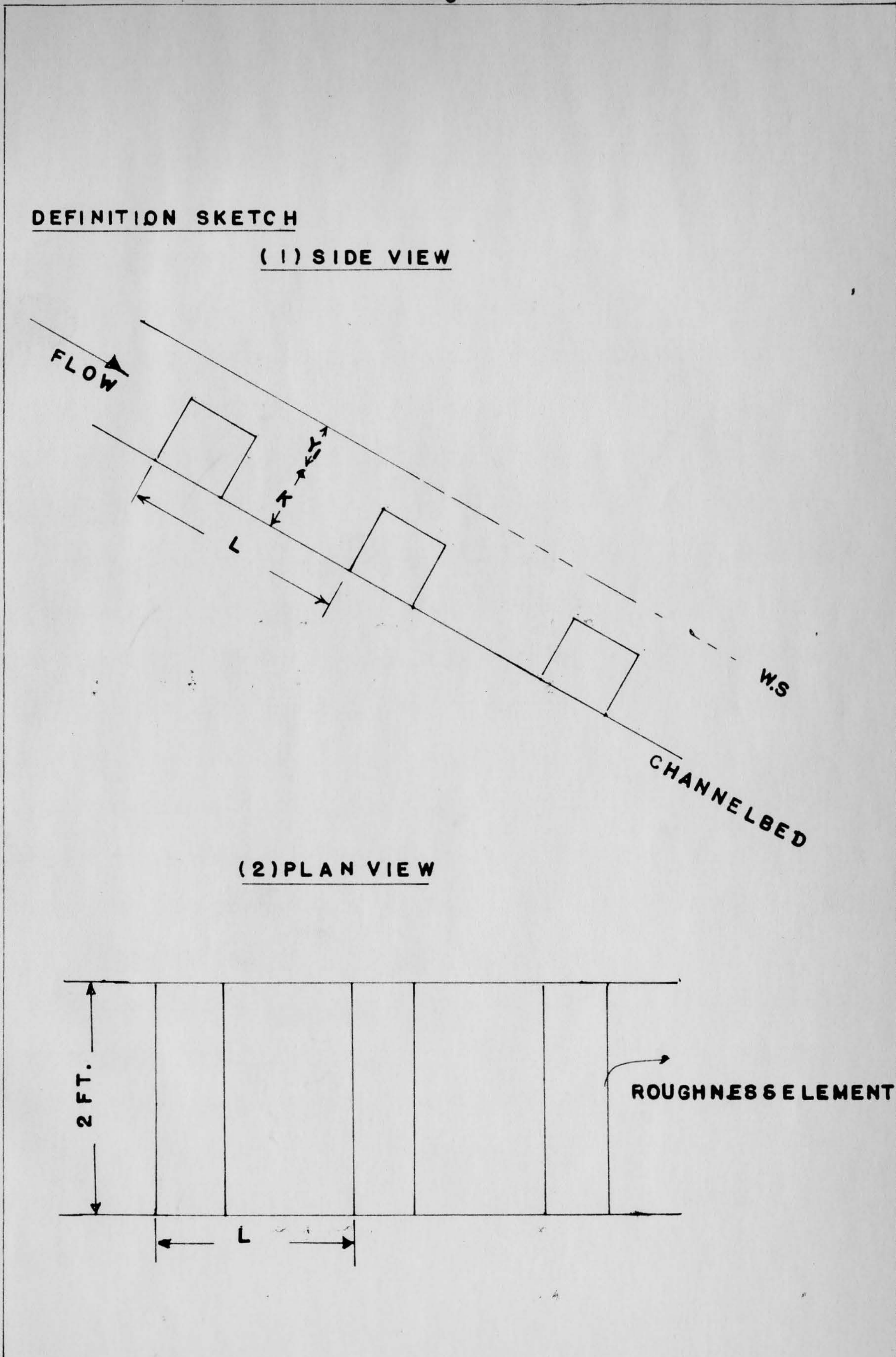
DEFINITION SKETCH
(1) SIDE VIEW
FLOW
Y
K
L
W.S
CHANNELBED
(2)PLAN VIEW
2 FT.
ROUGHNESS ELEMENT
L

Fig. I-1

II. REVIEW OF LITERATURE

The forces exerted on a solid body when fluid flows by belonged exclusively to the naval architect and aeronautical engineer. But now, all engineers find it necessary to become familiar with the fundamental mechanics of fluid motion. A knowledge of fluid resistance or drag has become of increasing importance in the design of buildings, bridges, automobiles, trains, airplanes, underwater craft and ships. The principles of lift are being applied with increasing importance in the design of turbines, propellers, and centrifugal pumps.

Drag Force. The idea of drag force is believed to have been introduced into hydraulic literature by DuBois (5) in 1879. However, the principle of balancing this force with the channel resistance in a uniform flow was started by Brahm (2) early in 1754. Leighley (8) attempted to determine the distribution of tractive force in channels of several shapes from data that had already been published on the velocity distribution in channel, but the results were not conclusive. Olesen and Florey (12) and others used the membrane analogy for determining the distribution of tractive force.

The concept of the three dimensional analysis of the tractive forces acting along a body resting on a slope of a channel and the gravity free is believed to have been given by Forchheimer (6), but a complete analysis of a channel section using this concept was first developed by Chia-Hwa Fan (4). The U. S. Bureau of Reclamation developed independently the analysis under the direction of E. W. Lane (9).

Chezy C. The first empirical formula that was adopted for velocity computation in smooth open channel was proposed by Antoine Chezy in 1775. Kutter and Ganguillet (7) believed that the French engineer, Chezy, was first to recognize the effect of boundary roughness on fluid flow. The formula proposed by Chezy was as follows:

$$V = C\sqrt{RS} \tag{II-1}$$

where V is the mean velocity of flow in feet, R is the hydraulic radius, S is the slope of the channel bed, and C is called Chezy's constant. This constant C was believed to depend on the slope of channel, the hydraulic radius, as well as the roughness of channel bed. Many investigators, among them Kutter and Ganguillet (7), developed formulae for the evaluation of C. For uniform flow in open channel the Chezy formula can be written as follows:

$$V = C\sqrt{R}\,\sqrt{S}$$

and the discharge Q:

$$Q = AC\sqrt{R}\,\sqrt{S} \tag{II-2}$$

where A is the cross-section area of channel, R and S as defined previously, and C, sometimes called Chezy resistance factor, is to be determined by means of the Ganguillet-Kutter, Bazin, Manning, or any other experimental or empirical formula.

Designating

$$A\, C\sqrt{R}\ \ S = K \qquad \text{(II-3)}$$

we obtain, instead of Eq. 3

$$Q = K\sqrt{S} \qquad \text{(II-4)}$$

and, therefore

$$S = \frac{Q^2}{K^2}$$

where K is called the conveyance of the cross-section. For a given channel, the value of (K) is a function of the depth y. This function can be traced as a curve $K = f(y)$, which curve features the capacity of the channel to convey water depending on the stage of flow.

When the friction factor, C, is determined by means of formula which does not contain S, such as Manning's or Bazin's formula, then in such case the conveyance curve features the capacity of a certain cross-section for the whole range of practically usable slope; in such case, C can be assumed to be constant. But if the Ganguillet-Kutter formula is used, the Chezy C may be considered as a variable which depends on the slope of the channel bed.

Drag Coefficient. The development of the concept of boundary layer started in 1904 with Prandtl (16). This concept provides a link between real fluid and ideal fluid. "For fluid having relatively small viscosity, the effect of internal friction in a fluid is appreciable only in a narrow region surrounding the fluid boundaries.* Within the boundary layer, relations may be computed from general equations for viscous fluids, but the momentum equation permits the development of approximate equations for boundary layer growth and drag.

The drag coefficient is defined:

$$F_D = C_D A \rho \frac{v^2}{2} \qquad \text{(II-5)}$$

in which A is the projected area of the body or roughness element, immersed in the fluid, on a plan perpendicular to the direction of flow, v is the mean velocity of the flow and C_D is the drag coefficient. It is known that C_D depends on Reynold's number as well as Mach's number. The effect of compressibility on the drag coefficient makes Mach's number more important than Reynold's number in gas flow.

III. DIMENSIONAL ANALYSIS

To find qualitative expression for the effective drag force offerred by a single two-dimensional roughness element dimensional analysis will be used.

The effective drag force offered by each roughness element can be expressed by:

$$F_D = f_1 (y_1, y_c, S, K, L, \rho g) \qquad \text{(III-1)}$$

where:

F_D = drag force in pounds

y_1 = the control depth on the upstream edge of roughness element

y_c = critical depth

S = slope of channel bed

K = height of roughness element

L = spacing of roughness elements

ρ = mass density of water

g = acceleration of gravity

Al-Khafaji (1) has shown that y_1, y_c and S are dependent on each other; therefore:

$$y_1 = f_2 (y_c, S) \qquad \text{(III-2)}$$

$$\text{or} \quad \frac{y_1}{y_c} = f_2 (S) \qquad \text{(III-3)}$$

Eq. 3 implies that for a given channel slope y_1 and y_c are dependent on each other, also for a given value of y_1 and y_c the slope is automatically determined. This fact simplifies and reduces Eq. 1 to the following three general functions:

$$F_D = f_3 (y_1, S, K, L, \rho, g) \qquad \text{(III-4)}$$

$$F_D = f_4 (y_c, S, K, L, \rho, g) \qquad \text{(III-5)}$$

$$F_D = f_5 (y_1, y_c, K, L, \rho, g) \qquad \text{(III-6)}$$

Using the pi-theorem on any one of Equations 4, 5, and 6, a number of dimensionless ratios are obtained and therefore a number of dimensionless functions are obtained. Eq. 5 reduces to the convenient form:

$$\frac{F_D}{\rho g K^3} = f_6 \left(S, \frac{y_c}{K}, \frac{L}{K}\right) \qquad \text{(III-7)}$$

To reduce the qualitative form of Eq. 7 into quantitative equation, laboratory data was used.

Letting Π_1 stand for $F_D/\rho g K^3$, Π_2 for S, Π_3 for L/K and Π_4 for y_c/K, therefore Eq. 7 may be written as:

$$\Pi_1 = f_6 (\Pi_2, \Pi_3, \Pi_4) \qquad \text{(III-8)}$$

IV. DRAG FORCE

In general the force exerted by the fluid on an immersed body in the direction of flow is called a drag force. A drag force is the summation of the components of all tangential and normal stresses on an immersed body. In case of streamlined bodies at high Reynold's numbers, the resultant effect of normal stresses will be minimum, and the drag can hence be considered due almost entirely to boundary-layer shear. In the case of bodies of angular profile, on the other hand, pressure drag or form drag outweighs the boundary shear drag that the total drag can be considered due almost entirely to form drag which is the unbalanced normal forces on the front and rear sides. The former case evidently approaches the limit of pure surface drag, and the latter the limit of pure form drag. Between these limits the proportionate effects of surface and form upon the total drag of a body can be evaluated only by measurement and integration of the pressure distribution. Pure form drag was considered dominant in this study.

In this chapter the drag force per single roughness will be evaluated in the rapid and tranquil flow regimes.

Relationships of Drag Forces

The drag force, F_D, is found to be a function of discharge, channel slope, and the geometry of the roughness elements of the channel bed.

A close observation of Table IV-1 reveals the fact that drag force always increases with discharge, channel slope, respectively.

TABLE IV-1

Comparison Between Measured and Computed Drag Force
In Rapid Flow (K = .135 x .135 ft.-bars)

$$F_D = 0.0169\ (S)^{.76}\ \left(\frac{L}{K}\right)^{1.13}\ \left(\frac{y_c}{K}\right)^{.86}$$

Run	Slope	Q	y_1	y_c	$\frac{L}{K}$	L	K	F_D meas.	F_D compt.	Deviat. %
7	2.56	.97	.181	.195	5	.675	.135	.346	.292	5.4
8	"	.935	.176	.190	"	"	"	.346	.286	6.0
9	"	1.20	.212	.225	"	"	"	.369	.330	3.9
10	"	1.48	.244	.260	"	"	"	.415	.374	4.1
8	5.18	1.25	.172	.230	"	"	"	.530	.574	4.4
9	"	1.57	.210	.270	"	"	"	.690	.659	3.2
6	12.18	.800	.125	.170	"	"	"	.840	.848	.8
7	"	.970	.130	.195	"	"	"	.920	.955	3.5
8	"	1.12	.145	.215	"	"	"	.990	1.04	5.0
9	"	1.40	.165	.250	"	"	"	1.070	1.175	10.5
5	8.253	.97	.135	.195	"	"	"	.693	.710	1.7
6	"	1.170	.150	.220	"	"	"	.806	.787	1.9
7	"	1.330	.165	.240	"	"	"	.830	.850	2.0
8	"	1.71	.195	.280	"	"	"	.900	.967	6.7
9	"	2.33	.235	.350	"	"	"	1.200	1.17	3.0
7	11.335	1.46	.240	.255	7.5	1.013	"	1.700	1.785	8.5
8	"	1.76	.225	.285	"	"	"	2.00	1.945	5.5
9	"	2.00	.238	.315	"	"	"	2.04	2.13	9.0
10	"	2.37	.255	.355	"	"	"	2.23	2.23	0.0
11	"	2.32	.280	.350	"	"	"	2.3	2.32	2.0
12	3.085	1.9	.295	.300	"	"	"	.782	.778	4.0
13	"	2.060	.312	.325	"	"	"	.784	.817	3.3
14	"	2.34	.335	.350	"	"	"	.785	.875	9.0
9	5.89	1.76	.243	.290	"	"	"	1.175	1.222	4.7
10	"	1.92	.253	.305	"	"	"	1.24	1.275	3.5
11	"	2.20	.275	.335	"	"	"	1.29	1.38	9.0
11	4.132	2.72	.328	.385	10	1.35	"	1.49	1.575	8.5
7	10.26	2.26	.260	.345	"	"	"	2.90	2.99	9.0
8	"	2.78	.275	.390	"	"	"	3.32	3.32	0.0
6	7.77	1.90	.287	.300	"	"	"	2.10	2.15	5.0
7	"	2.10	.270	.325	"	"	"	2.20	2.22	2.0
8	"	2.37	.284	.355	"	"	"	2.44	2.50	6.0
9	"	2.65	.300	.375	"	"	"	2.62	2.61	1
10	"	3.03	.320	.410	"	"	"	2.91	2.80	1

The drag force is also found to increase with increasing spacing and increasing size of roughness elements.

Development of Drag Force Equations

Eq. 8 of Chapter 3 is considered to develop the quantitative equations for the drag forces in rapid and tranquil flow regimes.

In the development of such equations the following general procedure was followed: (1) holding Π_3 and Π_4 constant the first component equation $(\Pi_1)_{3\,4}$, was obtained. (2) holding Π_2 and Π_4 constant, the second component equation $(\Pi_1)_{2\,4}$ was obtained. (3) holding Π_2 and Π_3 constant, the third component equation $(\Pi_1)_{2\,3}$ was obtained. (4) test of validity to see in what manner these component equations would combine was made in both developments, namely, in the rapid and tranquil flow regimes.

Drag Force Equation

In rapid flow regime. To obtain the prediction or quantitative equation, the component equations were first obtained and then combined properly.

Π_1 vs Π_2. For constant values of Π_3 and Π_4, Π_1 is related to Π_2 in the following manner.

$$\Pi_1 = C_1\,(\Pi_2)^{.76} \qquad \text{(IV-1)}$$

where C_1 is found to be 1.2 when Π_3 and Π_4 are 5 and 1.45 respectively as shown in Figure 4-1.

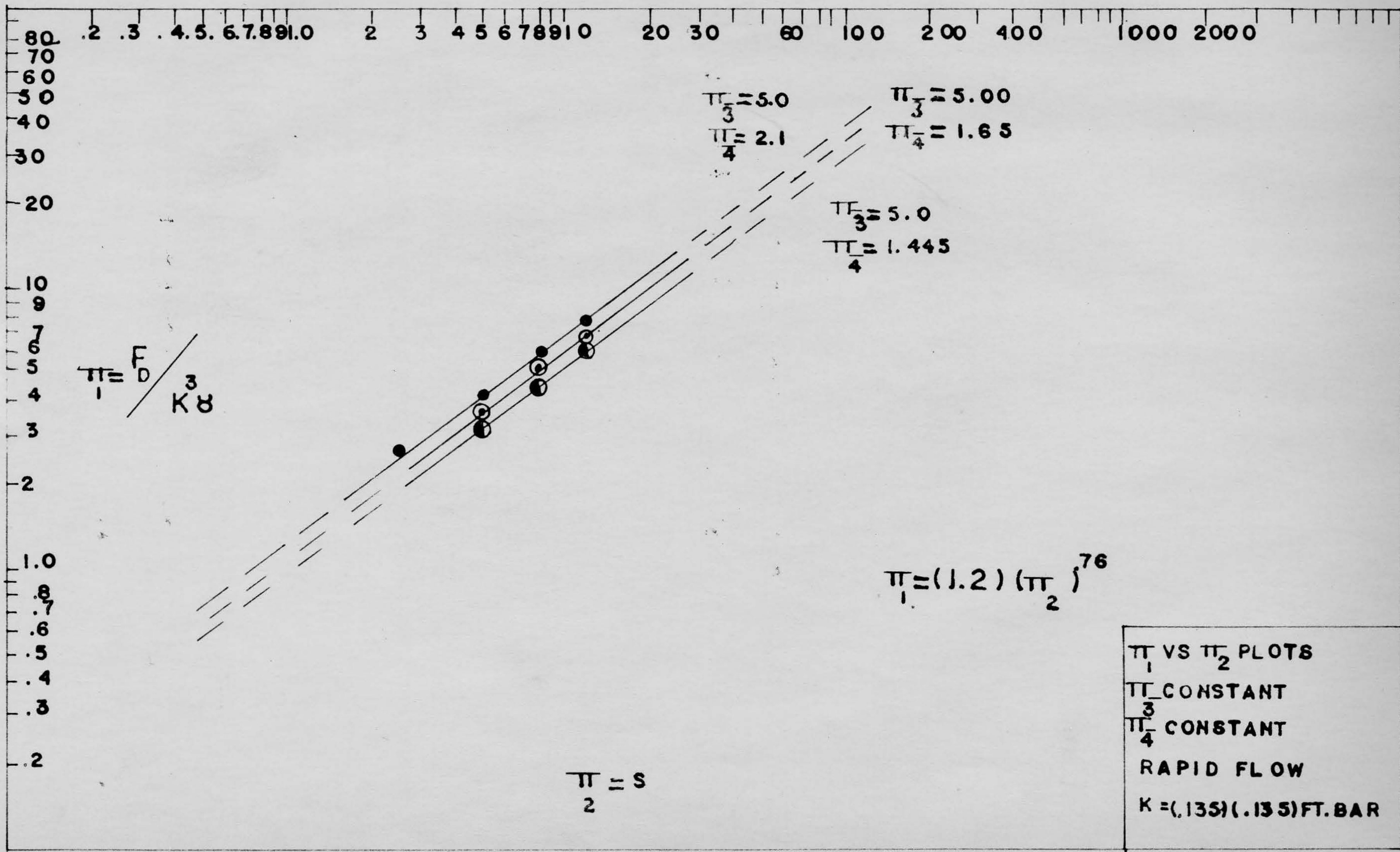
$\pi_3 = 5.0$
$\pi_4 = 2.1$
$\pi_3 = 5.00$
$\pi_4 = 1.65$
$\pi_3 = 5.0$
$\pi_4 = 1.445$
$\pi_1 = F_D / K\gamma^3$
$\pi_1 = (1.2)(\pi_2)^{.76}$
$\pi_2 = S$
π_1 VS π_2 PLOTS
π_3 CONSTANT
π_4 CONSTANT
RAPID FLOW
K =(.135)(.135) FT. BAR

Fig. IV-1

Π_1 vs Π_3. For constant values of Π_2 and Π_4, the second component equation relating Π_1 and Π_4 is found to be

$$\Pi_1 = C_2\,(\Pi_3)^{1.13} \qquad \text{(IV-2)}$$

where C_2 is 1.2 when Π_2 and Π_3 have the constant values of 11 and 2.1 respectively as shown in Figure 4-2.

Π_1 vs Π_4. For constant values of Π_2 and Π_3, third component equation is found to be

$$\Pi_1 = C_3\,(\Pi_4)^{.86} \qquad \text{(IV-3)}$$

where C_3 is 4.2 when $_2$ and $_3$ have the constant values of 11 and 5 respectively as shown in Figure 4-3.

Π_1 vs all Π's. To obtain the general prediction equation, the component equations 1, 2 and 3 were properly combined. The final prediction equation is found to be

$$F_D = 0.0169\,(S)^{.76}\left(\frac{L}{K}\right)^{1.13}\left(\frac{y_c}{K}\right)^{.86} \qquad \text{(IV-4)}$$

where Eq. 4 is only valid for the .135 x .135 ft. roughness elements.

Eq. 4 was used to compute the drag forces as listed in Table IV-1. These computed values compared satisfactorily with those measured F_D as shown in Table IV-1.

Drag Force Equations in Tranquil Flow Regime

Two prediction equations were derived in this regime, one for the .135 x .135 ft. bars and one for the .3 x .3 ft. bars. The development

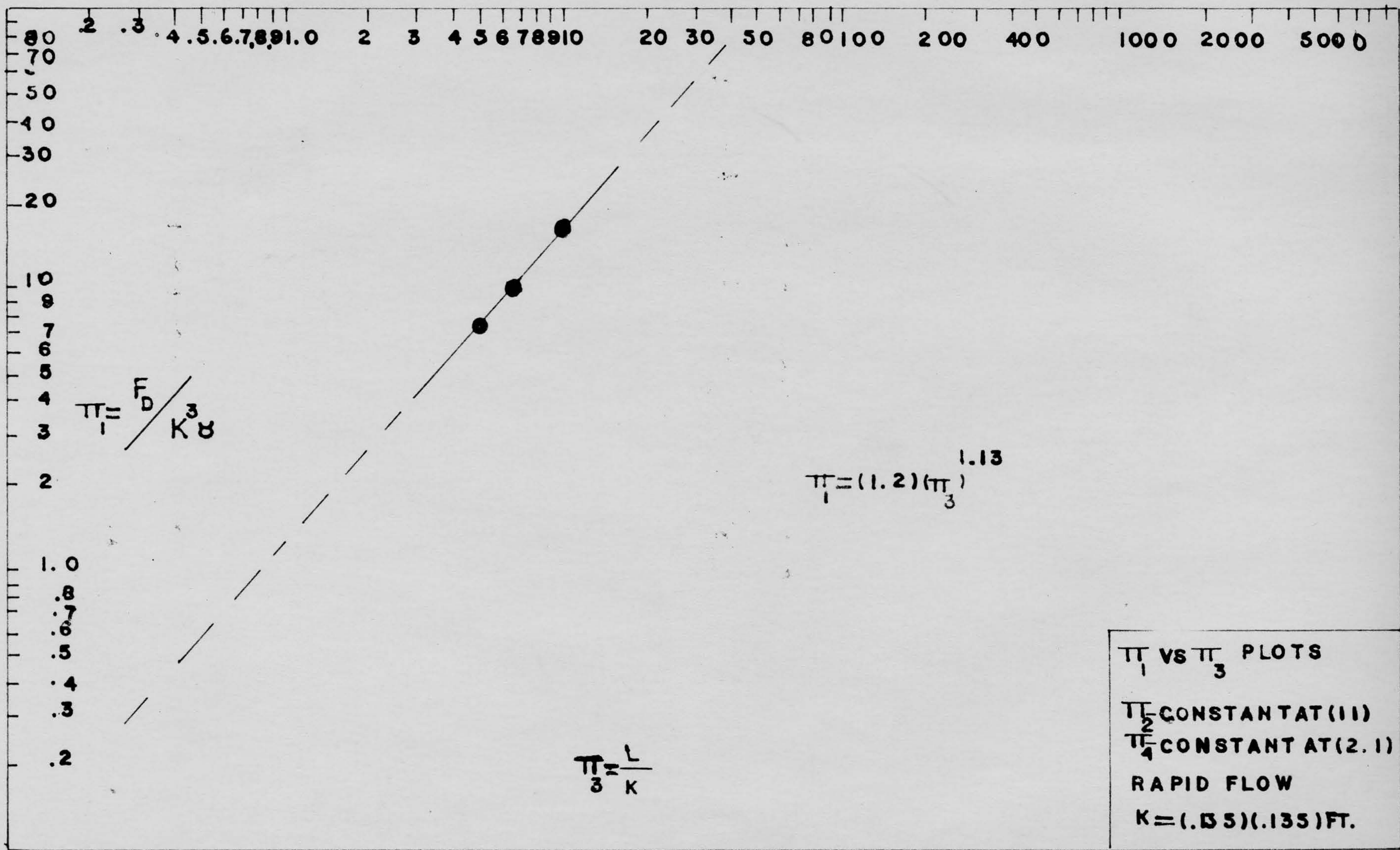

.2 .3 .4 .5 .6 .7 .8 .9 1.0 2 3 4 5 6 7 8 9 10 20 30 50 80 100 200 400 1000 2000 5000
80 70 50 40 30 20 10 9 7 6 5 4 3 2 1.0 .8 .7 .6 .5 .4 .3 .2
$\pi_1 = F_D / K^3 \gamma$
$\pi_1 = (1.2)(\pi_3)^{1.13}$
$\pi_3 = \frac{L}{K}$
π_1 VS π_3 PLOTS
π_2 CONSTANT AT (11)
π_4 CONSTANT AT (2.1)
RAPID FLOW
K = (.135)(.135) FT.

Fig. IV-2

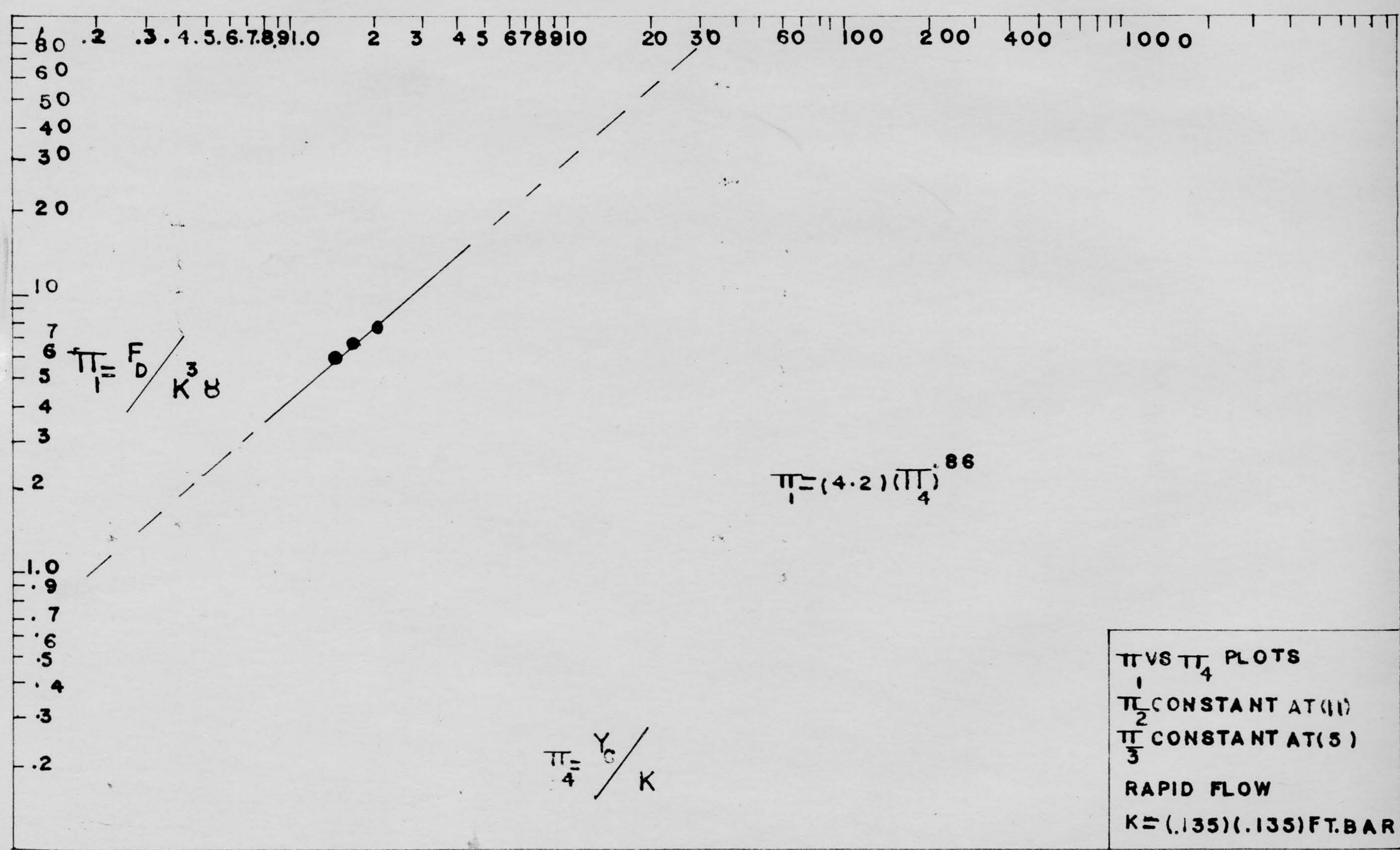
$\pi_1 = F_D / K^3 \gamma$
$\pi_4 = Y_c / K$
$\pi_1 = (4.2)(\pi_4)^{.86}$
π_1 VS π_4 PLOTS
π_2 CONSTANT AT (11)
π_3 CONSTANT AT (5)
RAPID FLOW
K = (.135)(.135) FT. BAR

Fig. 1V-3

of these equations are similar to that in rapid flow regime. The component equations for the .135 x .135 ft. bars are shown in Figures 4-4, 4-5, and 4-6 respectively. And those for the .3 x .3 ft. bars are shown in Figures 4-7, 4-8, and 4-9 respectively.

The general equation for the .135 x .135 ft. bars was found to be

$$F_D = 0.0167\,(S)^{.665}\,(\frac{L}{K})^{1.57}(\frac{y_c}{K})^{.615} \qquad \text{(IV-5)}$$

and that for the .3 x .3 ft. bars was found to be

$$F_D = .316\,(S)^{.495}(\frac{L}{K})^{.73}(\frac{y_c}{K})^{1.02} \qquad \text{(IV-6)}$$

Eq. 5 and Eq. 6 were used to compute the drag forces and the computed drag forces compared well with those measured as shown in Tables IV-2 and IV-3.

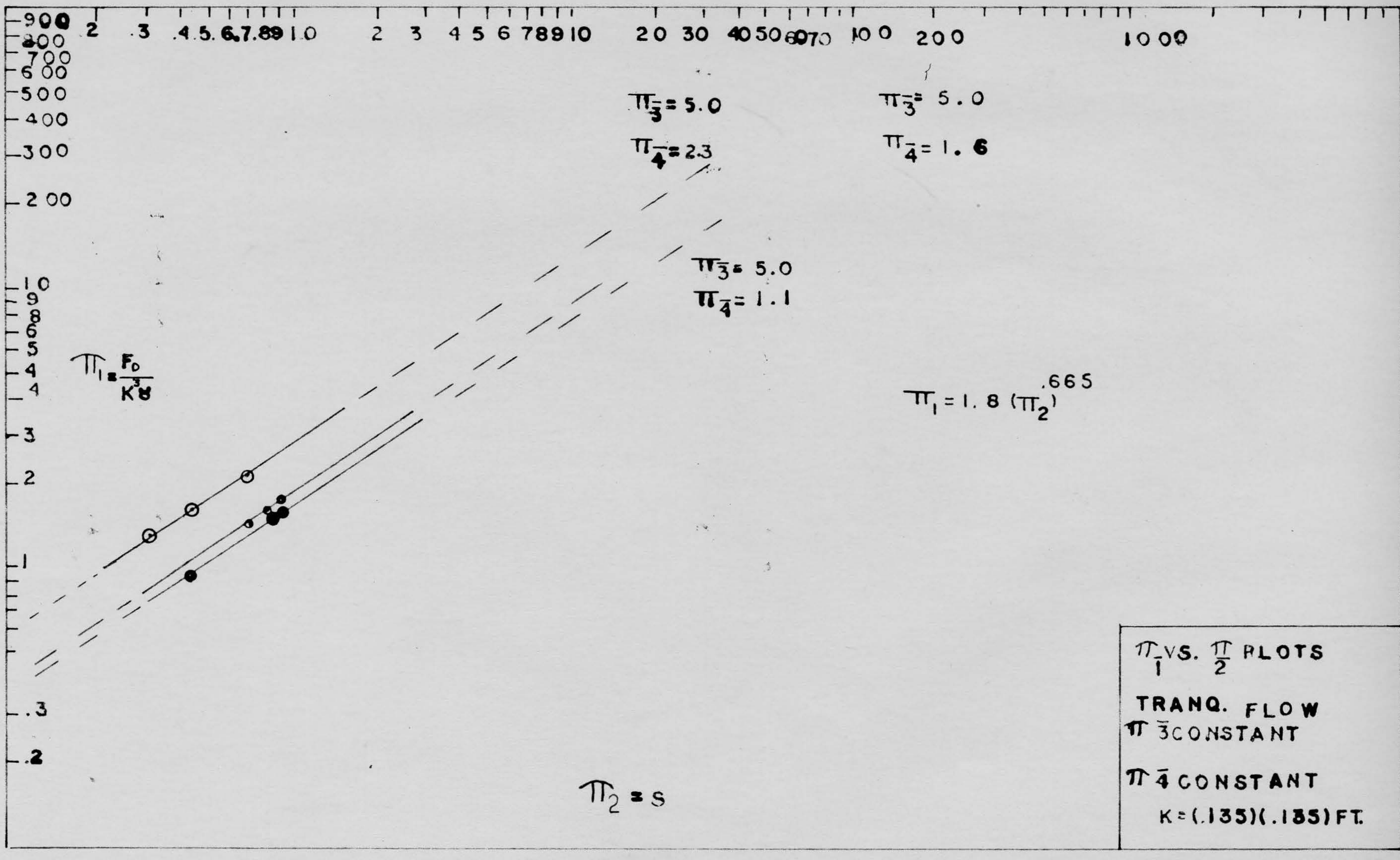

$\Pi_3 = 5.0$
$\Pi_4 = 2.3$
$\Pi_3 = 5.0$
$\Pi_4 = 1.6$
$\Pi_3 = 5.0$
$\Pi_4 = 1.1$
$\Pi_1 = \frac{F_0}{K^3 \gamma}$
$\Pi_1 = 1.8 (\Pi_2)^{.665}$
$\Pi_2 = S$
Π_1 VS. Π_2 PLOTS
TRANQ. FLOW
Π_3 CONSTANT
Π_4 CONSTANT
K = (.135)(.135) FT.

Fig. IV-4

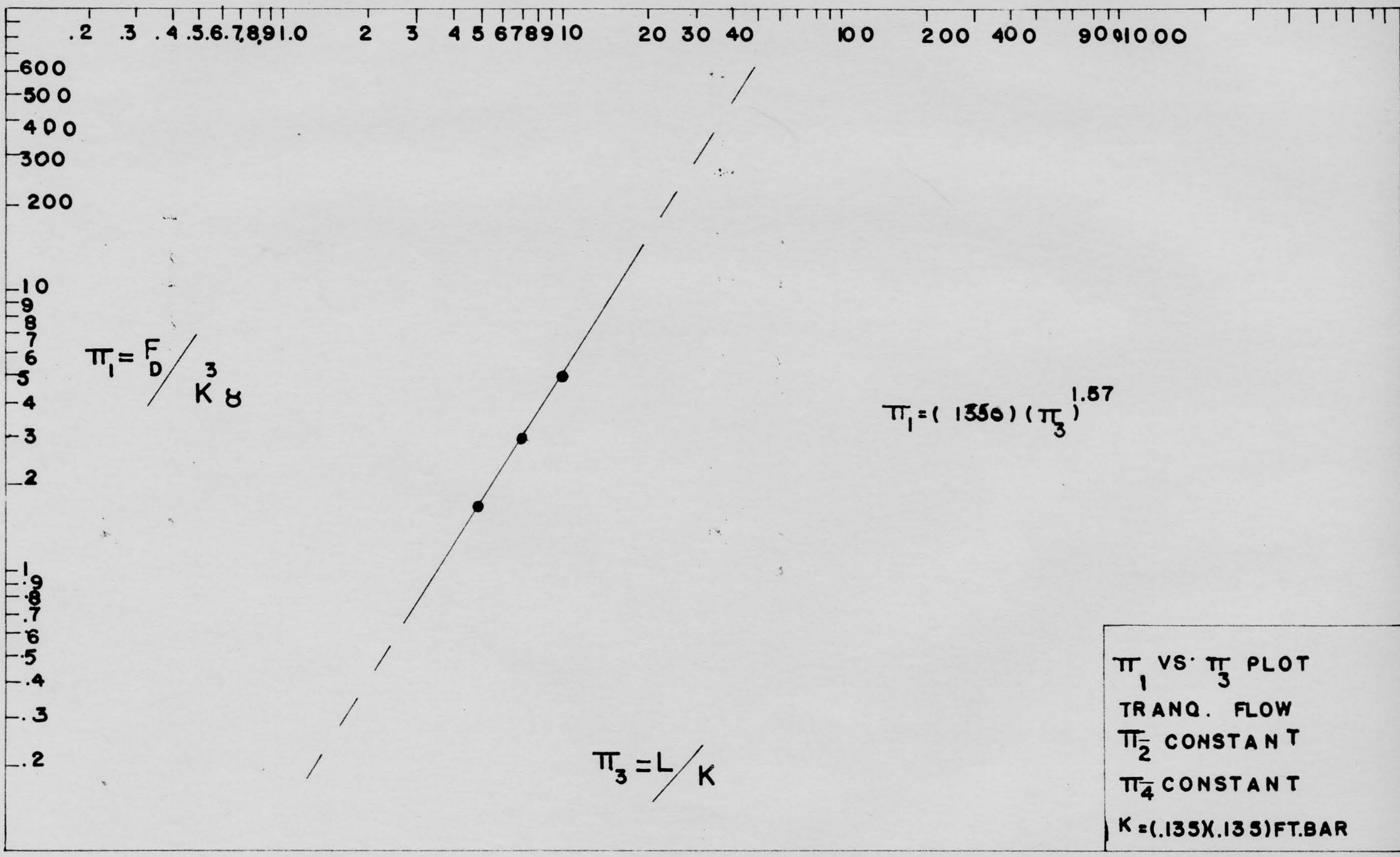

.2 .3 .4 .5 .6 .7 .8 .9 1.0 2 3 4 5 6 7 8 9 10 20 30 40 100 200 400 900 1000
600
500
400
300
200
10
9
8
7
6
5
4
3
2
1
.9
.8
.7
.6
.5
.4
.3
.2
$\pi_1 = F_D / K^3 \gamma$
$\pi_1 = (.1350)(\pi_3)^{1.57}$
$\pi_3 = L / K$
π_1 VS. π_3 PLOT
TRANQ. FLOW
π_2 CONSTANT
π_4 CONSTANT
K =(.135)(.135) FT. BAR

Fig. IV-5

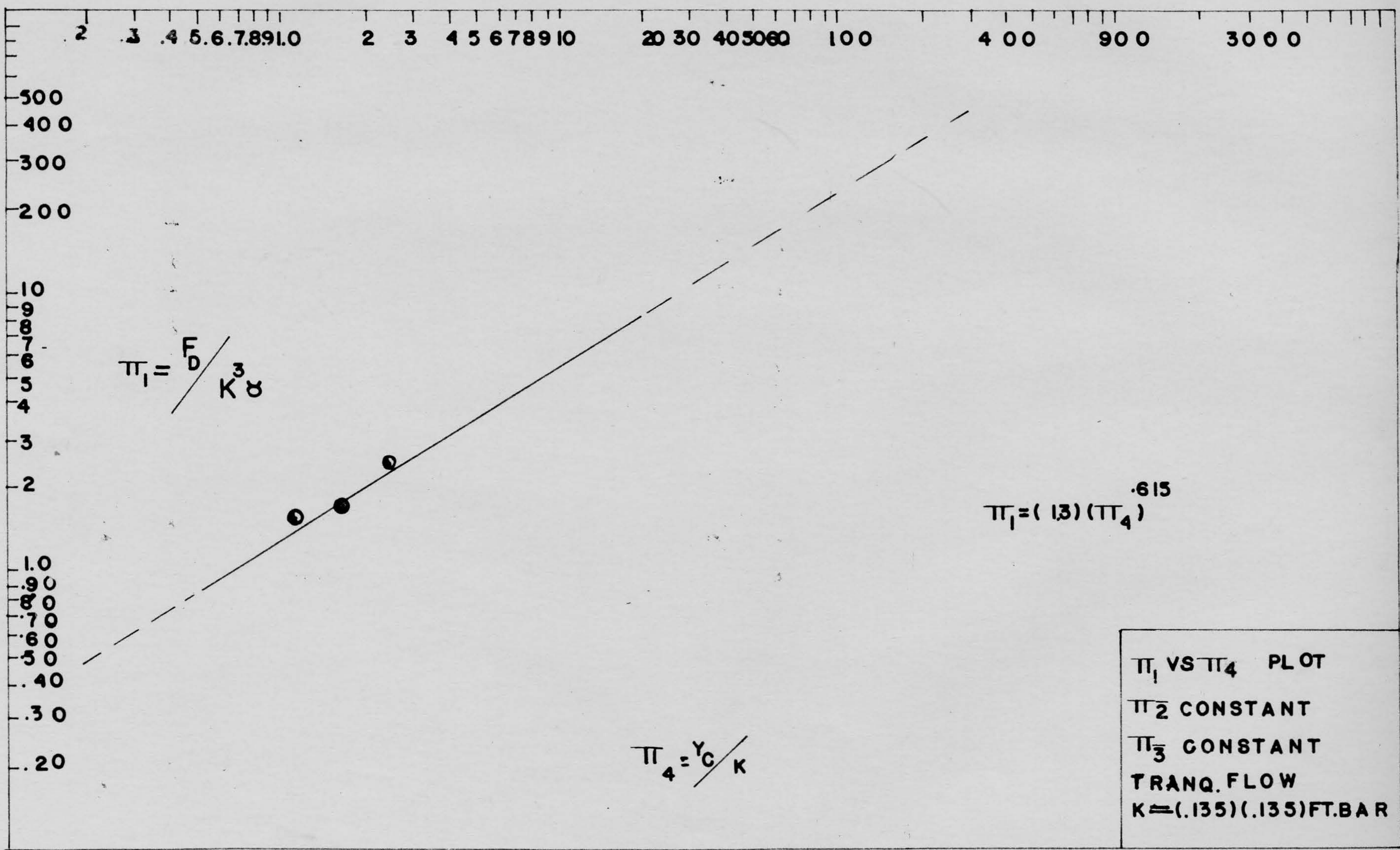

2 .3 .4 5 .6 .7 .8 .9 1.0 2 3 4 5 6 7 8 9 10 20 30 40 50 60 100 400 900 3000
500 400 300 200 10 9 8 7 6 5 4 3 2 1.0 .90 .80 .70 .60 .50 .40 .30 .20
$\Pi_1 = F_D / K^3 \gamma$
$\Pi_1 = (1.3)(\Pi_4)^{.615}$
$\Pi_4 = Y_C / K$
Π_1 VS Π_4 PLOT
Π_2 CONSTANT
Π_3 CONSTANT
TRANQ. FLOW
K=(.135)(.135) FT. BAR

Fig. IV-6

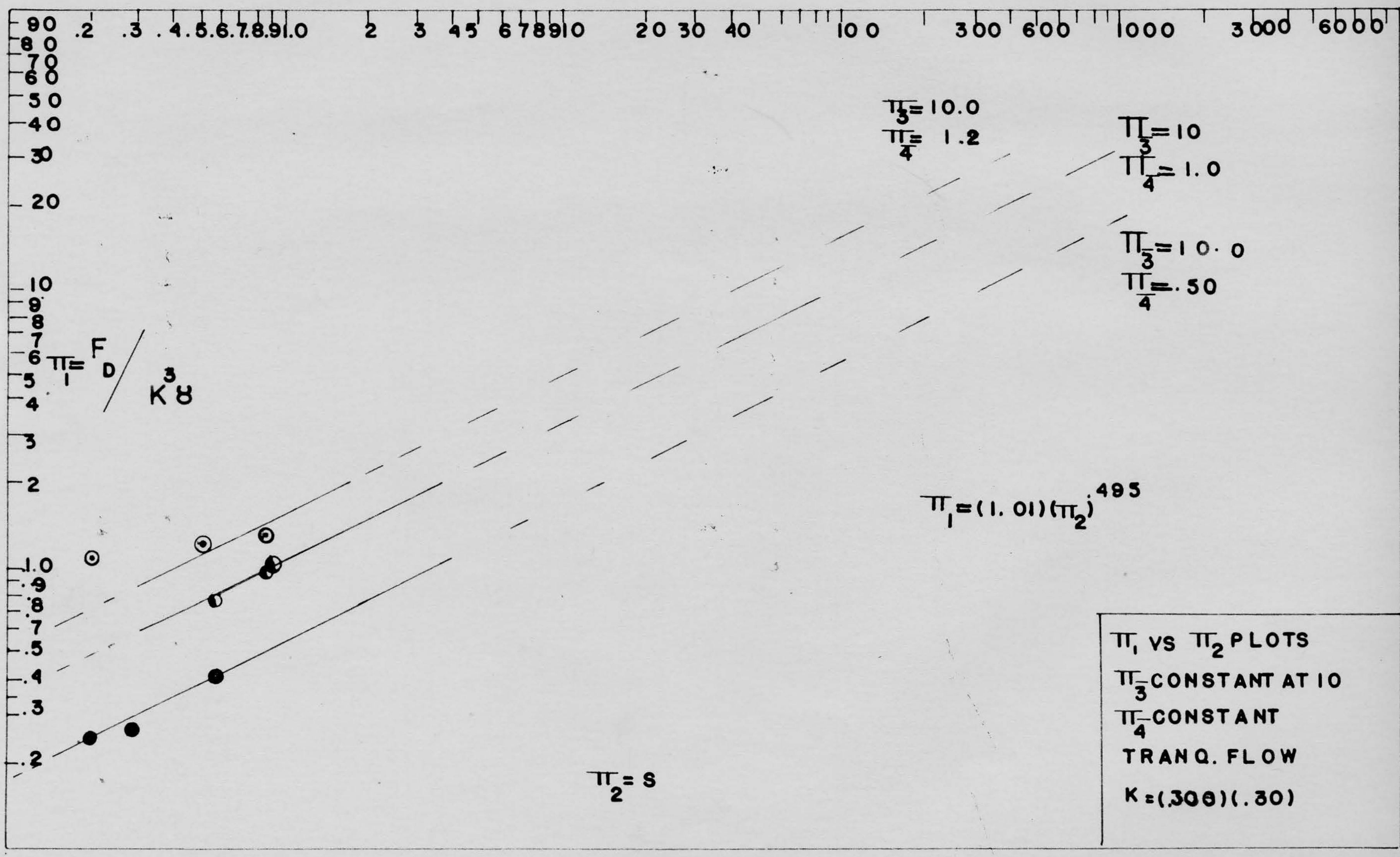
$\Pi_1 = F_D / K^3 \delta$
$\Pi_3 = 10.0$
$\Pi_4 = 1.2$
$\Pi_3 = 10$
$\Pi_4 = 1.0$
$\Pi_3 = 10.0$
$\Pi_4 = .50$
$\Pi_1 = (1.01)(\Pi_2)^{.495}$
$\Pi_2 = S$
Π_1 VS Π_2 PLOTS
Π_3 CONSTANT AT 10
Π_4 CONSTANT
TRANQ. FLOW
K = (.308)(.30)

Fig. IV-7

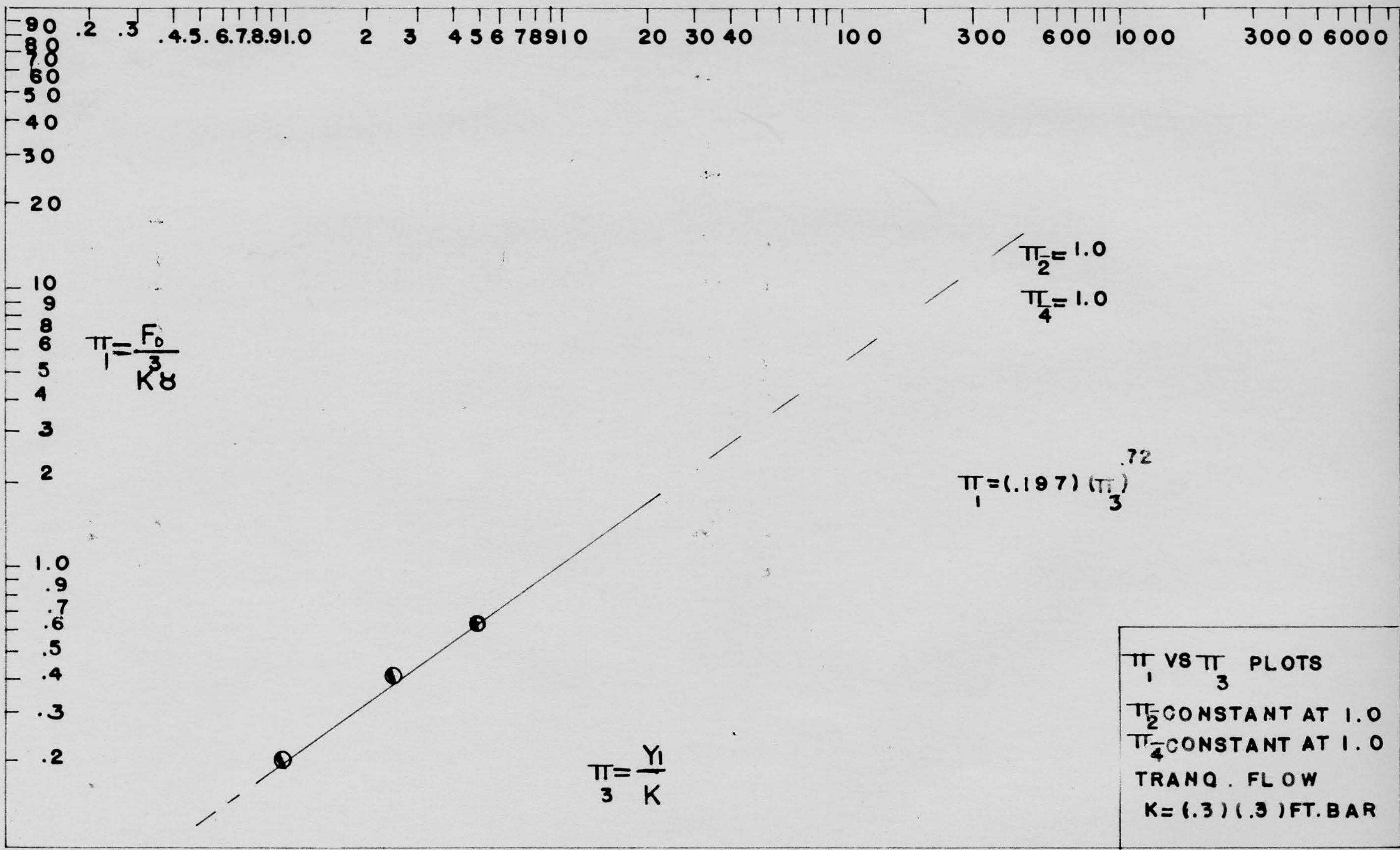

.2 .3 .4.5. 6.7.8.9 1.0 2 3 4 5 6 7 8 9 10 20 30 40 100 300 600 1000 3000 6000
90 80 70 60 50 40 30 20 10 9 8 6 5 4 3 2 1.0 .9 .7 .6 .5 .4 .3 .2
$\pi_1 = \frac{F_0}{K^3 \gamma}$
$\pi_2 = 1.0$
$\pi_4 = 1.0$
$\pi_1 = (.197)(\pi_3)^{.72}$
$\pi_3 = \frac{Y_1}{K}$
π_1 VS π_3 PLOTS
π_2 CONSTANT AT 1.0
π_4 CONSTANT AT 1.0
TRANQ. FLOW
K= (.3)(.3) FT. BAR

Fig. lV-8

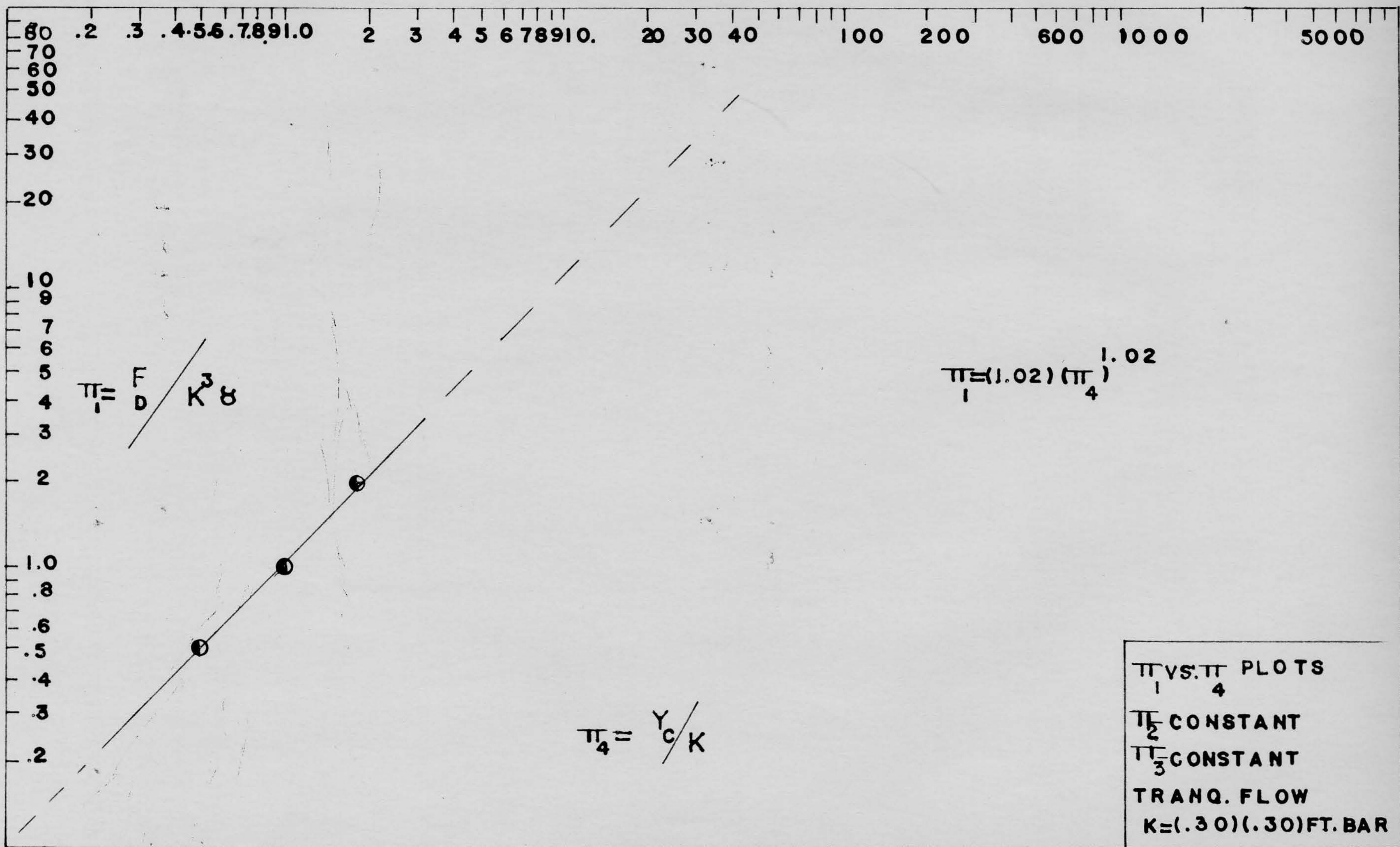

$\pi_1 = F_D / K^3 \gamma$
$\pi_4 = Y_c / K$
$\pi_1 = (1.02)(\pi_4)^{1.02}$
π_1 VS. π_4 PLOTS
π_2 CONSTANT
π_3 CONSTANT
TRANQ. FLOW
K=(.30)(.30)FT. BAR

Fig. 1V-9

TABLE IV-2

Comparison Between Measured and Computed Drag Force
In Tranquil Flow (K = .135 x .135 ft. bars)

$$F_D = 0.0167\,(S)^{.665}\left(\frac{L}{K}\right)^{1.57}\left(\frac{y_o}{K}\right)^{.615}$$

Run	Slope	Q	y_1	y_o	$\frac{L}{K}$	L	K	F_D meas.	F_D compt.	Deviat. %
1	.33	.675	.200	.1485	5	.675	.292	.167	.106	36.50
2	"	.970	.255	.194	"	"	"	.177	.1245	29.40
3	"	1.28	.298	.233	"	"	"	.161	.1395	13.40
4	"	1.8	.357	.291	"	"	"	.206	.161	19.90
1	.73	.75	.210	.159	"	"	"	.152	.189	23.30
2	"	1.12	.252	.214	"	"	"	.220	.225	2.27
3	"	1.40	.300	.248	"	"	"	.280	.246	12.10
4	"	1.76	.340	.288	"	"	"	.236	.270	14.40
1	.985	.850	.215	.172	"	"	"	.254	.231	9.05
2	"	1.170	.246	.219	"	"	"	.262	.278	6.10
3	"	1.46	.285	.254	"	"	"	.296	.304	2.7
4	"	2.00	.348	.316	"	"	"	.304	.348	14.5
1	.46	.675	.200	.149	"	"	"	.1435	.132	8.02
2	.11	1.17	.270	.214	"	"	"	.203	.1655	18.5
3	"	1.530	.318	.262	"	"	"	.232	.1875	19.2
4	"	1.920	.370	.308	"	"	"	.262	.207	21.0
5	"	2.400	.415	.355	"	"	"	.338	.225	35.0
1	.91	.580	.165	.136	"	"	"	.237	.187	22.4
2	"	1.04	.248	.204	"	"	"	.253	.252	.395
3	"	1.28	.270	.233	"	"	"	.279	.274	1.79
4	"	1.98	.358	.314	"	"	"	.296	.329	11.2
1	1.75	.935	.198	.190	"	"	"	.312	.373	19.55
3	"	2.00	.298	.273	"	"	"	.350	.466	33.2
1	.17	.88	.263	.182	7.5	1.013	"	.245	.146	40.4
1	.405	.63	.202	.142	"	"	"	.253	.238	5.96
3	"	1.12	.295	.214	"	"	"	.390	.308	21.0
4	"	1.40	.322	.248	"	"	"	.342	.336	1.75
5	"	1.61	.350	.272	"	"	"	.455	.356	21.80
1	.87	.85		.174	10	1.35	"	.760	.648	14.75
1	.63	.675	.195	.149	"	"	"	.444	.482	8.55
2	.63	1.20	.282	.224	"	"	"	.532	.621	16.75
3	"	1.62	.320	.273	"	"	"	.620	.700	13.70
4	"	1.85	.350	.294	"	"	"	.770	.741	3.77
1	.355	.75	.205	.159	"	"	"	.280	.343	22.5
2	"	.935	.247	.192	"	"	"	.351	.385	9.70
3	"	1.33	.307	.239	"	"	"	.505	.441	12.70

TABLE IV-3

Comparison Between Measured and Computed Drag Force
In Tranquil Flow (K = .3 x .3 ft. bars)

$$F_D = .316\,(S)^{.495}\left(\frac{L}{K}\right)^{.72}\left(\frac{y_o}{K}\right)^{1.02}$$

Run	Slope	Q	y_1	y_o	$\frac{L}{K}$	L	K	F_D meas.	F_D compt.	Deviat. %
1	.5	.750	.250	.160	5	1.46	.292	.440	.40	9.1
2	"	1.46	.491	.255	"	"	"	.530	.622	17.35
3	"	2.00	.55	.315	"	"	"	.993	.775	11.9
4	"	2.45	.51	.360	"	"	"	.998	.884	11.4
5	"	3.40	.712	.450	"	"	"	.994	1.112	11.9
1	.43	1.80	.406	.295	"	"	"	.607	.607	0.0
1	1.15	.87	.237	.180	"	"	"	.680	.660	2.94
1	.84	.63	.341	.145	7.5	2.16	"	.660	.605	8.34
3	"	1.70	.534	.280	"	"	"	1.20	1.185	1.25
1	.285	.53	.393	.130	10.0	2.92	"	.412	.390	5.34
1	.56	.65	.203	.150	"	"	"	.655	.631	3.73
1	.15	.75	.384	.165	"	"	"	.388	.364	6.20
1	.84	.97	.396	.195	"	"	"	1.070	1.011	5.50
2	"	1.61	.478	.270	"	"	"	1.540	1.42	7.80
1	.47	.675	.393	.155	"	"	"	.552	.600	8.70
1	.87	1.2	.463	.225	"	"	"	1.260	1.19	5.56
2	"	1.46	.495	.255	"	"	"	1.450	1.355	6.55
3	"	1.85	.545	.300	"	"	"	1.590	1.605	.95
4	"	2.23	.593	.340	"	"	"	1.780	1.814	1.91
1	.26	.625	.414	.145	"	"	"	.625	.418	1.71
2	.38	1.26	.303	.230	2.5	.73	"	.322	.297	7.76
4	"	2.23	.381	.340	"	"	"	.537	.447	18.1
2	1.00	1.24	.278	.230	"	"	"	.515	.483	6.20
3	"	1.78	.310	.290	"	"	"	.656	.610	7.12
1	.37	.58	.172	.140	"	"	"	.276	.1765	36.1
2	"	.935	.235	.190	"	"	"	.303	.241	20.8
2	.54	1.17	.248	.220	2.54	.74	"	.363	.351	3.31
3	"	1.66	.305	.270	"	"	"	.566	.428	24.40
3	1.03	1.51	.296	.260	"	"	"	.634	.556	12.30
1	.49	.75	.227	.165	5	1.46	"	.368	.395	7.34
2	"	1.17	.289	.220	"	"	"	.571	.530	7.2
3	"	1.85	.375	.300	"	"	"	.738	.729	1.22
1	1.14	.985	.239	.195	"	"	"	.644	.625	2.95
2	"	1.20	.252	.225	"	"	"	.592	.723	22.2
3	"	1.94	.365	.310	"	"	"	.978	1.000	2.25

V. CHEZY AND DRAG COEFFICIENTS

Evaluation of flow velocity, discharge and drag forces are of prime importance in any hydraulic analysis concerning conduits. For such evaluation the Chézy and drag coefficients are usually required.

In this chapter a quantitative study of both the Chézy and drag coefficient is made. Graphical correction between the two is also obtained.

Chézy Coefficient, C

Due to lack of adequate data at the time, Chézy believed C to be a constant which later proved not to be the case. The majority of investigators are of the opinion that C can be a function of one or a combination of Reynold number, channel slope, hydraulic radius and the geometry of roughness of the channel bed. Due to this variability the interrelationships between C and other variables need to be clarified.

Realizing the fact that Chézy formula is restricted to relatively smooth channel immediately raises the question: Is then the Chézy formula and therefore C valid for extremely rough channels as is the case in this investigation? In answer to this question Al-Khafaji derived a modified Chézy equation (14,15) from basic considerations and therefore showed that the conventional C should be modified to reflect the existence of the form drag forces imposed by the bed roughness elements against the channel flow. The modified Chézy formula is:

$$V = C/\left(\frac{PL\gamma}{PL\gamma RS - F_D}\right)^{\frac{1}{2}} \qquad \text{(V-1)}$$

For relatively smooth channel the form drag is negligible and Eq. 1 reduces to the conventional Chézy equation:

$$V = C/\sqrt{\frac{1}{RS}} = C\sqrt{RS} \qquad \text{(V-2)}$$

Realizing that the term (PL RS) is the gravity component of the weight of water in the direction of flow, then Eq. 1 may be written in this form:

$$V = C/\left(\frac{PL\,\gamma}{WS-F_D}\right)^{\frac{1}{2}} \qquad \text{(V-3)}$$

where V is the mean velocity of flow, W is the weight of water between any two roughness elements, S the slope of channel bed, F_D the drag force per single roughness element, C is the modified Chézy constant, P the wetted perimeter, L the spacing of roughness element and γ is the specific weight of water.

Eq. 3 may be written in the following form:

$$C^2 = (PL\,\gamma)/(WS - F_D)\,(V^2) \qquad \text{(V-4)}$$

Letting $\epsilon = PL\gamma$, Eq. 4 reduces to

$$C^2 = \frac{V^2\,\epsilon}{WS - F_D} \qquad \text{(V-5)}$$

C_m vs $(V^2)/(WS - F_D.)$ Realizing that ϵ varies with spacing L, ϵ was held constant at different levels and the plot of Figure 5-1 was made. From this figure it is clear that C increases with L/K. It is to be noted if it were not for the existance of roughness elements in the channel bed, Eq. 5 would have been reduced to the conventional

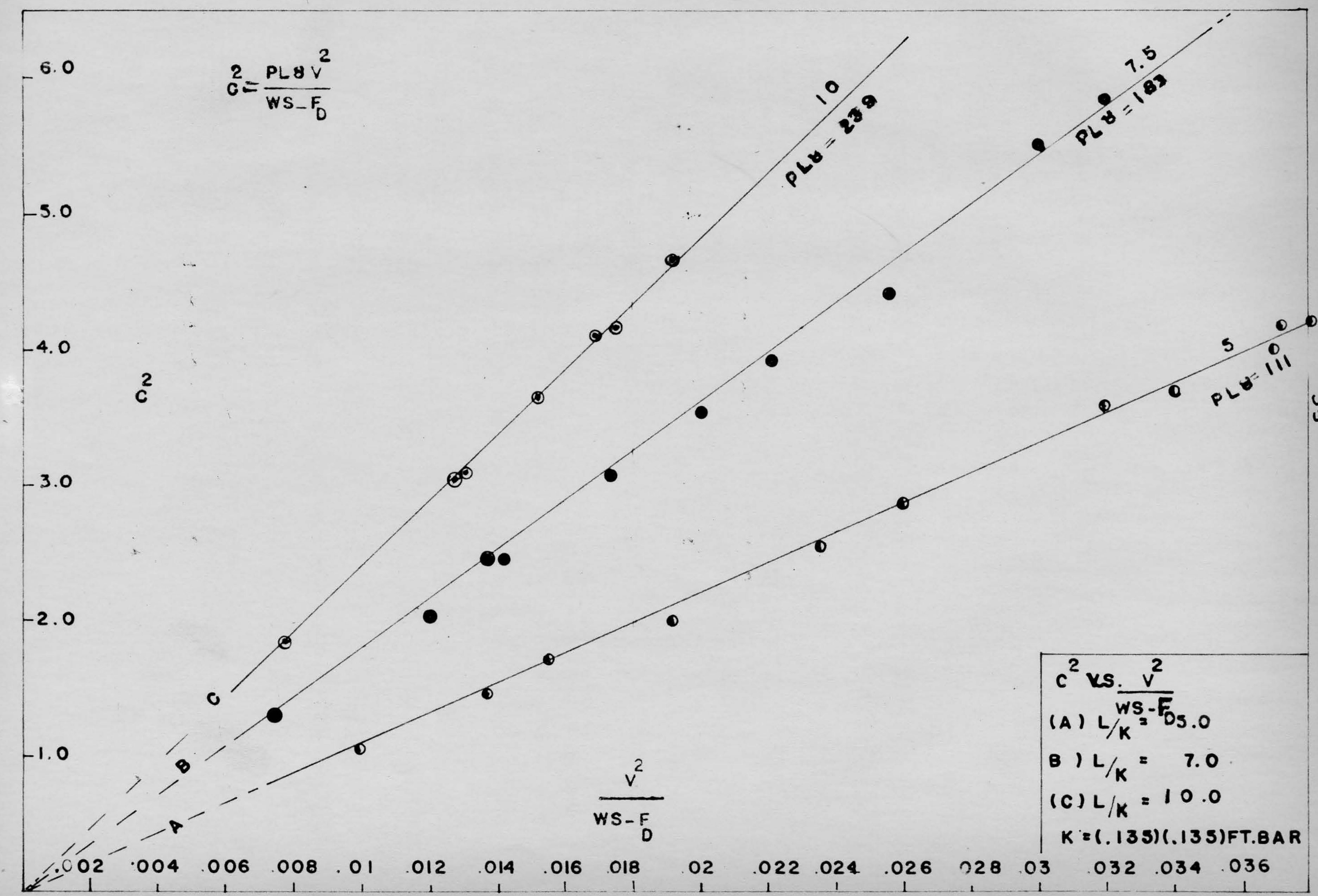

$C^2 = \frac{PL\delta V^2}{WS - F_D}$
6.0
5.0
4.0
3.0
2.0
1.0
C^2
10
PLδ = 239
7.5
PLδ = 183
5
PLδ = 111
C
B
A
$\frac{V^2}{WS - F_D}$
.002 .004 .006 .008 .01 .012 .014 .016 .018 .02 .022 .024 .026 .028 .03 .032 .034 .036
C^2 VS. $\frac{V^2}{WS-F_D}$
(A) L/K = 5.0
B) L/K = 7.0
(C) L/K = 10.0
K = (.135)(.135) FT. BAR

Fig. V-1

Chézy formula:

$$C^2 = \frac{V^2}{RS} \tag{V-6}$$

and that would have caused all three curves to converge into one simple curve.

C_m vs L/K. To study the relationship between C and the relative spacing, L/K, plot of Figure V-2 was made. From this plot it is clear that C increases with L/K. This is in agreement with finding of Al-Khafaji (1) and Sabir (15). This fact is indeed obvious from Figure V-1 also. It is to be noted that Sabir (15) indicated that at lower values of L/K there is a tendency for C to decrease up to a limiting value of L/K. This decreasing tendency is indeed inconclusive and further study in that region must be conducted.

To plot Figure V-2 C_D was held constant at three different levels and C/ g was plotted against L/K.

C_m vs y_1/K. Relationship between C and the control depth, y, is shown in Figure V-3. From this figure it is clear that C increases with depth.

Relationship between C and total depth $y_1 + K$ is shown in Figure V-4. From this figure it is clear that C increases with $y_1 + K/K$ for constant value of L/K. To plot Figure V-4, L/K was held constant at different levels and C/ g was plotted against $y_1 + K/K$.

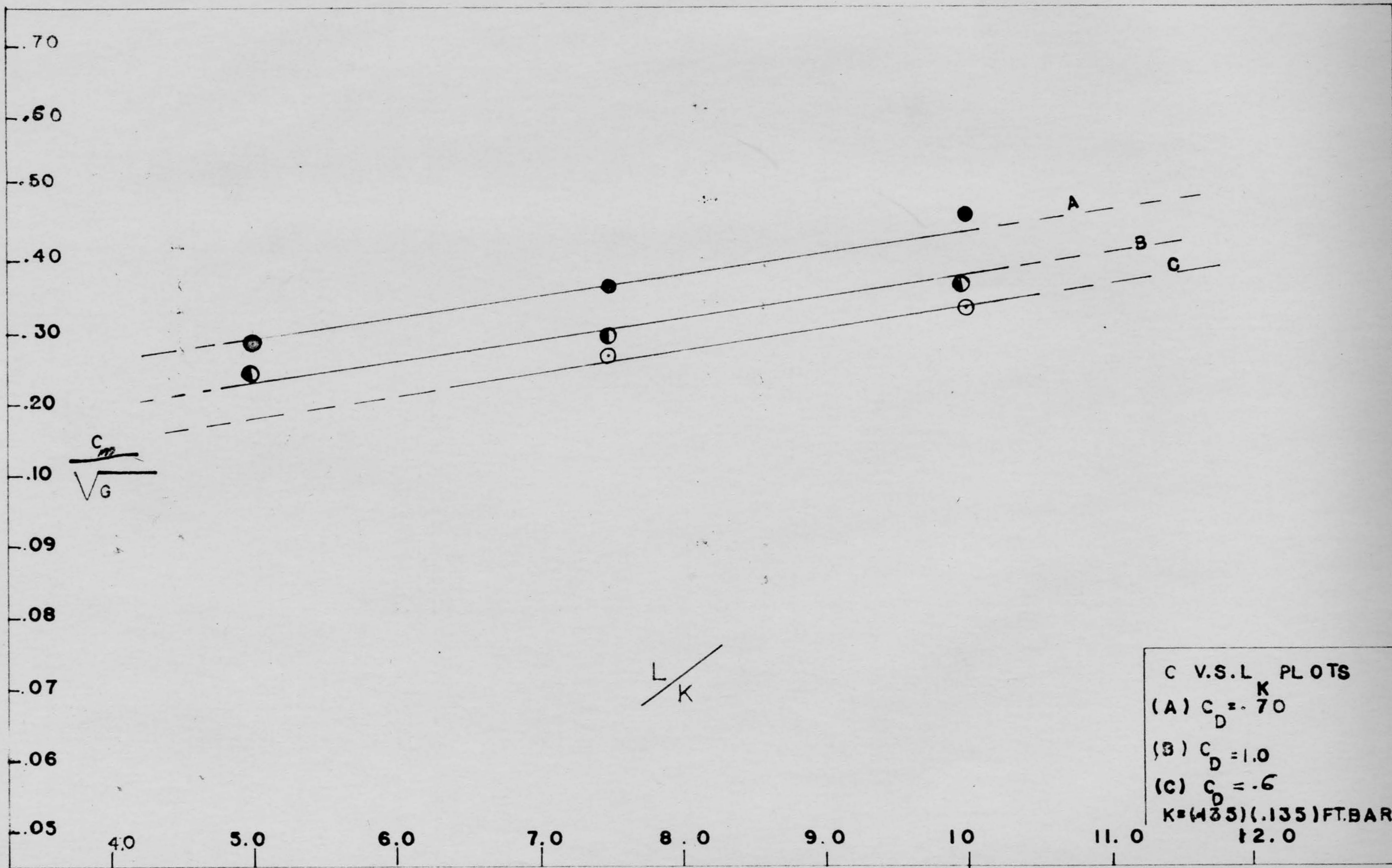
.70
.60
.50
.40
.30
.20
.10
.09
.08
.07
.06
.05
4.0
5.0
6.0
7.0
8.0
9.0
10
11.0
12.0
A
B
C
$\frac{C_m}{\sqrt{G}}$
L/K
C V.S. L/K PLOTS
(A) C_D = .70
(B) C_D = 1.0
(C) C_D = .6
K=(.135)(.135) FT. BAR

Fig. V-2

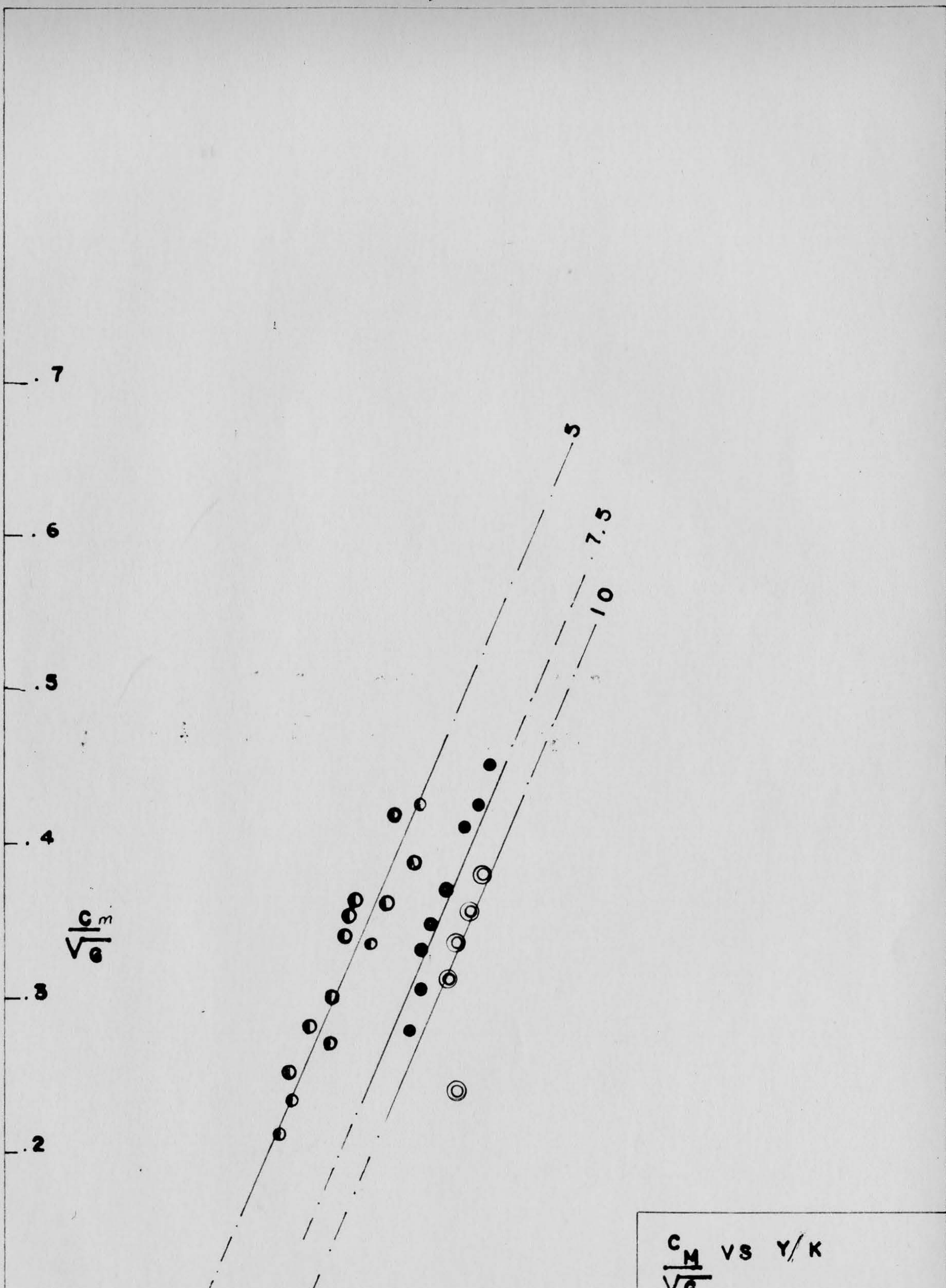
.7
.6
.5
.4
.3
.2
.1
$\frac{C_m}{\sqrt{G}}$
5
7.5
10
Y_1/K
.4 .5 .6 .7 .8 .9 1 2 3 4 5 6 7 8 9 10
$\frac{C_M}{\sqrt{G}}$ VS Y/K
A) L / K = 5.0
B) L / K = 7.50
C) L / K = 10.0

Fig. V-3

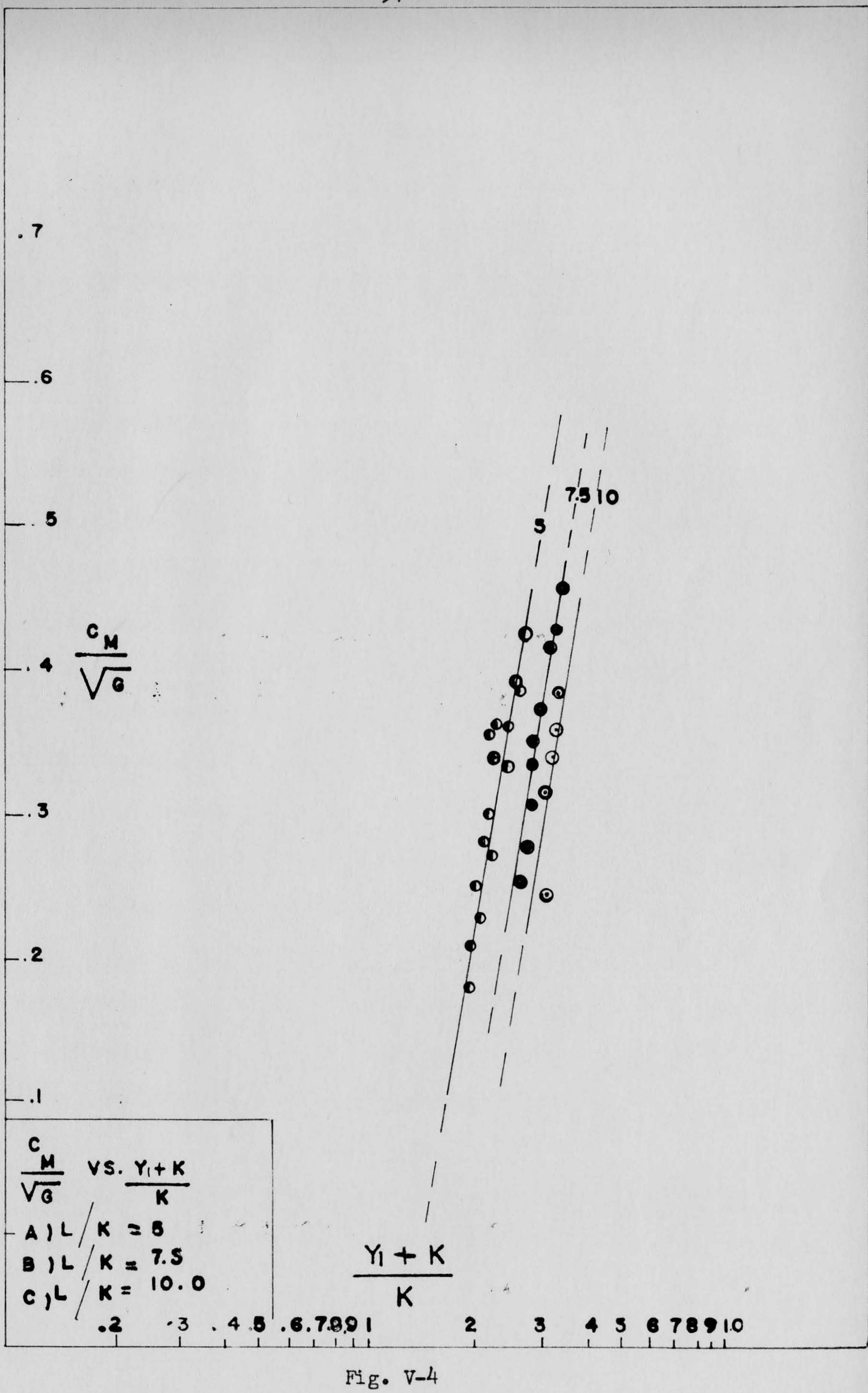
.7
.6
.5
.4
.3
.2
.1
$\frac{C_M}{\sqrt{G}}$
7.5
10
5
$\frac{C_M}{\sqrt{G}}$ VS. $\frac{Y_1+K}{K}$
A) L/K = 5
B) L/K = 7.5
C) L/K = 10.0
$\frac{Y_1 + K}{K}$
.2
.3
.4
.5
.6
.7
.8
.9
1
2
3
4
5
6
7
8
9
10

Fig. V-4

Drag Coefficient

The drag coefficient, C_D, represents a measure of resistance to flow. A drag force is usually expressed in terms of C_D, dynamic pressure and the projected area normal to the flow direction:

$$F_D = C_D A \rho \frac{V^2}{2} \qquad (V\text{-}7)$$

The behavior of C_D with respect to the modified Chézy C, and the relative spacing L/K, was studied. Also to facilitate the solution of the modified Chézy formula a graph of WS vs F_D was made. It is to be noted that C_D was computed by Eq. 7.

C_D vs L/K. A plot of C_D vs L/K was made in Figure V-5. From this figure it is shown that C_D increases with relative spacing, L/K; this is understandable since F_D increases with L/K. To plot Figure V-5 C_D and S were held constant.

C_D vs C. Holding L/K as constant at three different levels, C_D was plotted against C/ g, Figure V-6, V-7. C_D was also plotted against the modified Chézy coefficient, C, as derived by Al-Khafaji (1).

C_{1D} vs C_1. The variation of C_1 with C_{1D} was also studied for constant values of L/K. It is seen from Figure V-8 that C_1 decreases with increasing values of C_{1D}. It is also clear that C_1 increases when the relative spacing, L/K, increases.

Chézy C, Modified C_m and C_1

The Chézy constant C was computed and the modified coefficient C_m wad determined. These values are tabulated with C_1 values for the same

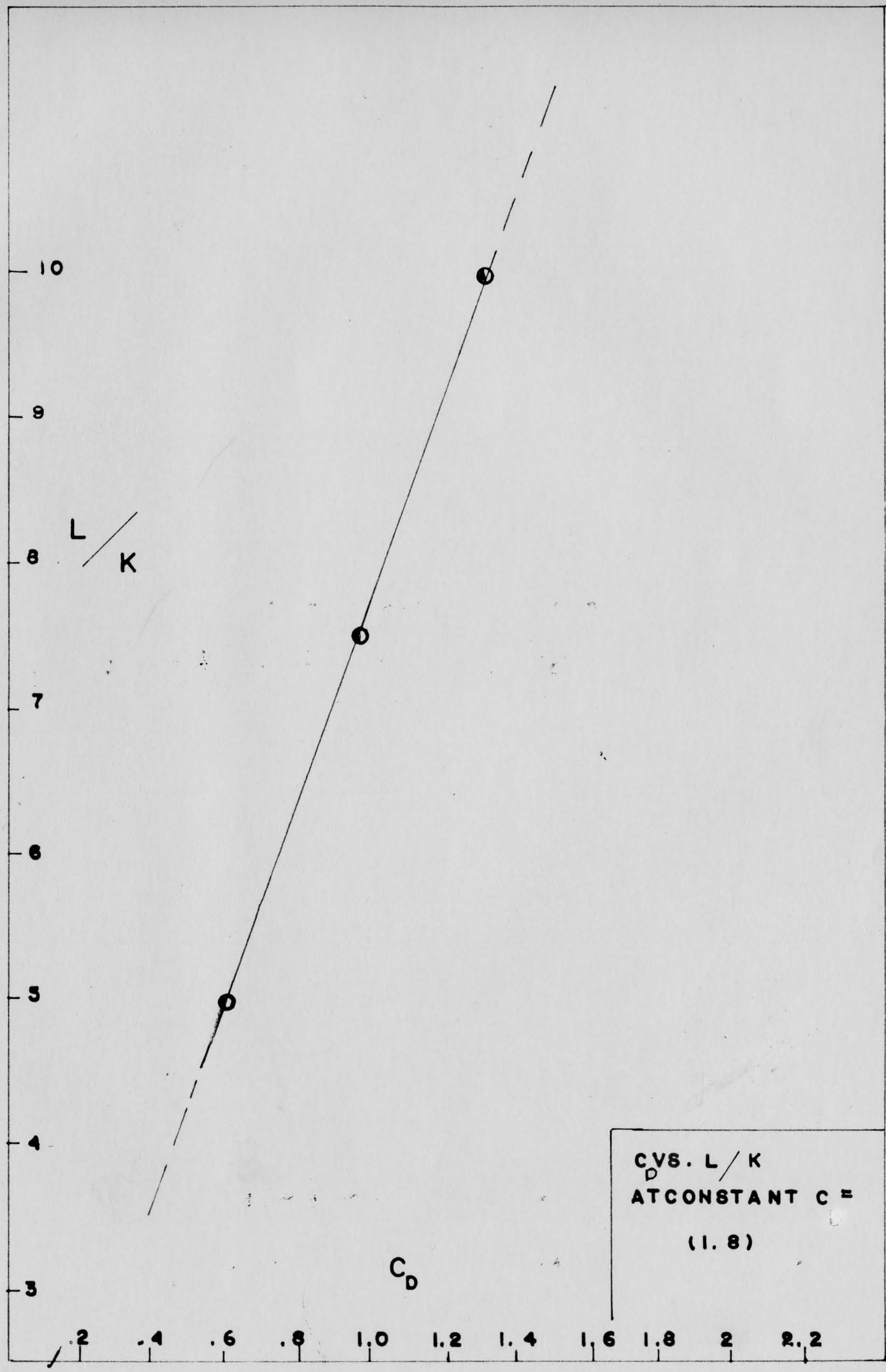

Fig. V-5

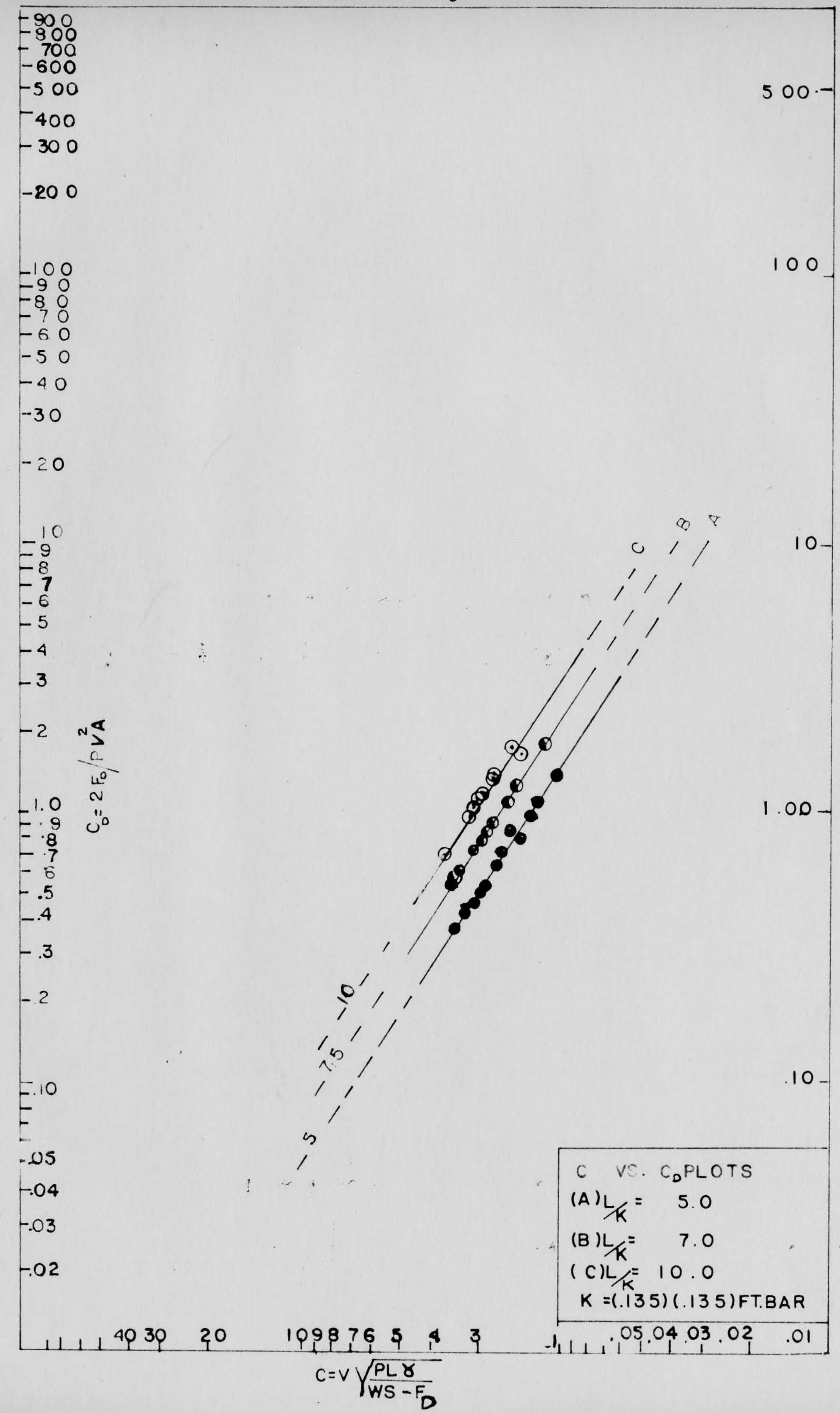

$C_D = 2F_D / \rho V^2 A$
$C = V\sqrt{\frac{PL\gamma}{WS - F_D}}$
C VS. C_D PLOTS
(A) L/K = 5.0
(B) L/K = 7.0
(C) L/K = 10.0
K = (.135)(.135) FT. BAR

Fig. V-6

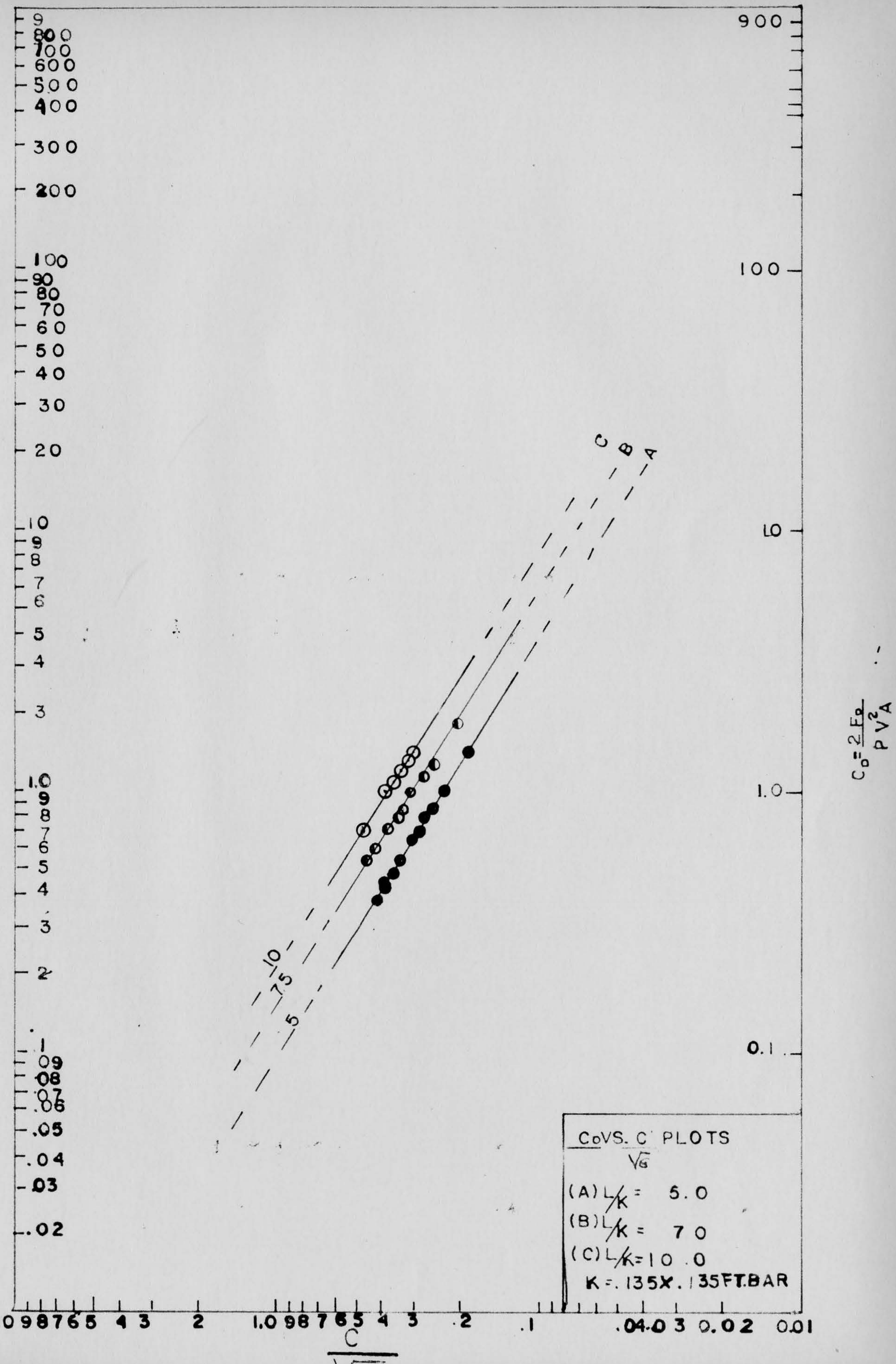

$C_D = \frac{2 F_D}{\rho V^2 A}$
C
B
A
10
7.5
5
C_D VS. $\frac{C}{\sqrt{G}}$ PLOTS
(A) L/K = 5.0
(B) L/K = 7 0
(C) L/K = 10 .0
K = .135X.135FT.BAR
$\frac{C}{\sqrt{G}}$

Fig. V-7

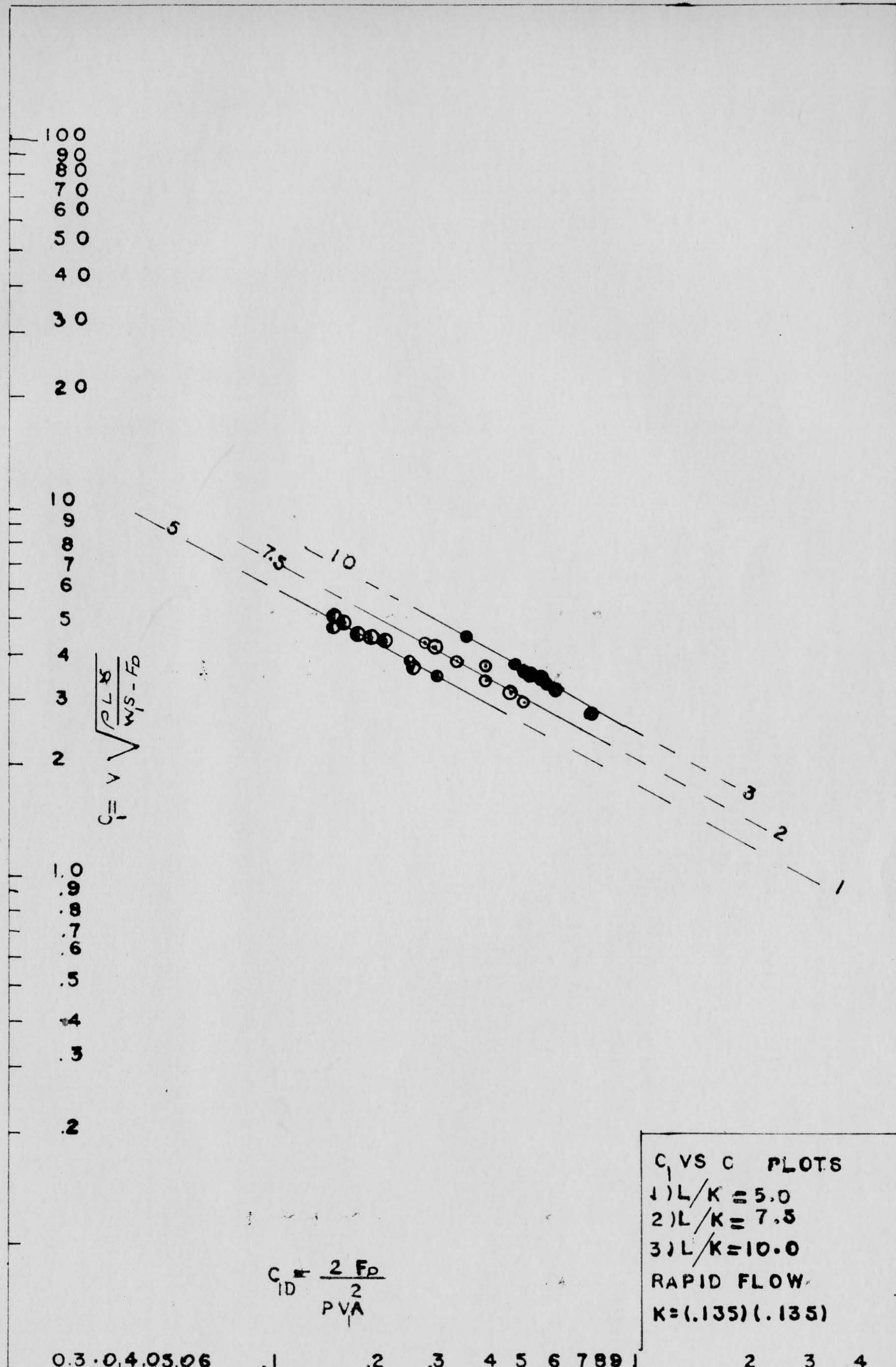
100
90
80
70
60
50
40
30
20
10
9
8
7
6
5
4
3
2
1.0
.9
.8
.7
.6
.5
.4
.3
.2
5
7.5
10
3
2
1
C₁ VS C PLOTS
1) L/K = 5.0
2) L/K = 7.5
3) L/K = 10.0
RAPID FLOW
K = (.135)(.135)
0.3 .04 .05 .06 .1 .2 .3 .4 .5 .6 .7 .8 .9 1 2 3 4

Fig. V-8

geometric and hydraulic conditions for the purpose of comparing them. Table V-5 shows the results obtained.

F_D vs WS

Computed values of F_D were plotted against WS values with L/K held as constant, Figure V-9. It is clear that F_D increases with the slope of the channel and the weight of the water between two consecutive roughness elements. Tables V-1, 2, 3, 4, 5 show the results as computed.

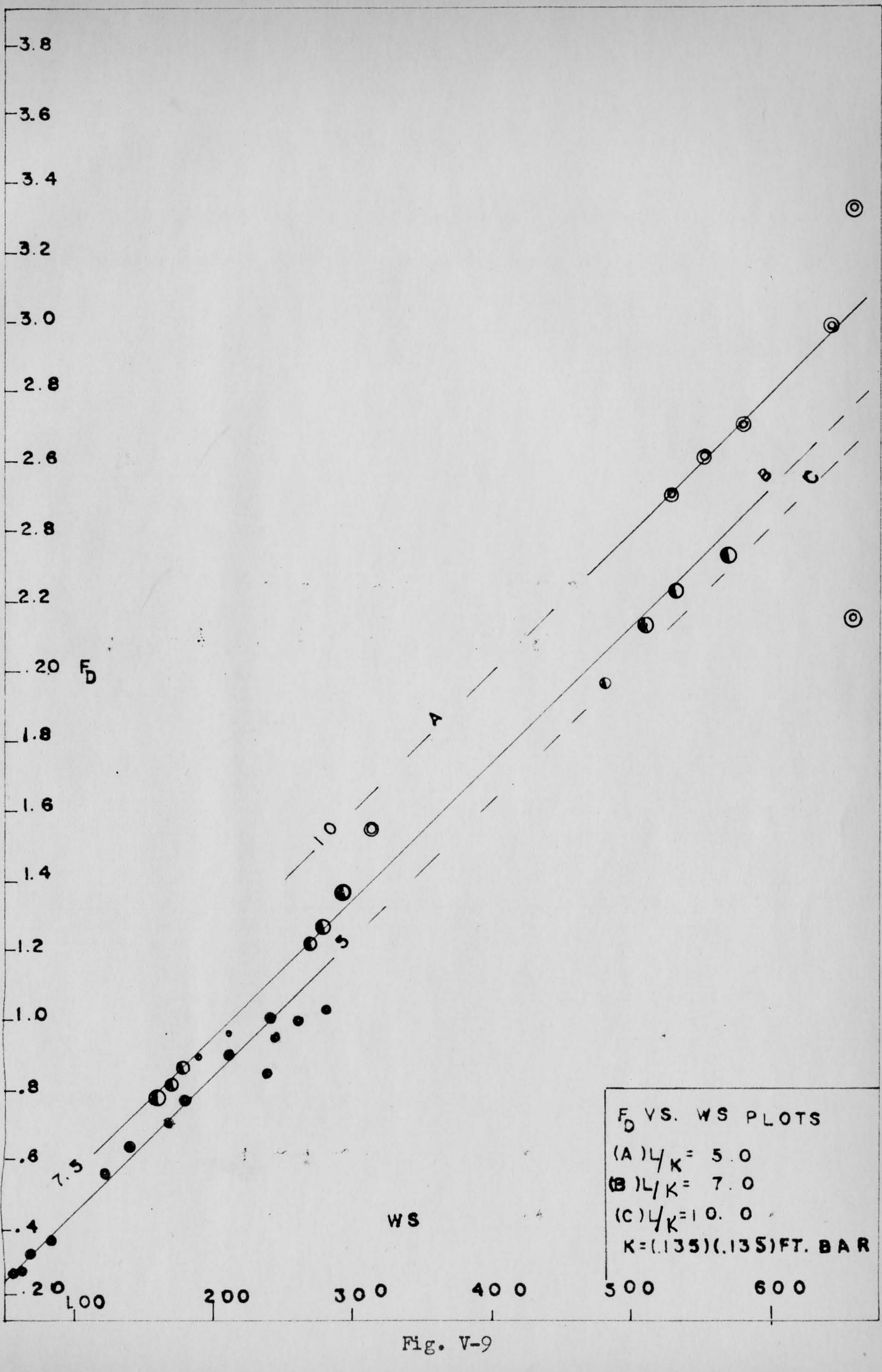
3.8
3.6
3.4
3.2
3.0
2.8
2.6
2.8
2.2
.20
F_D
1.8
1.6
1.4
1.2
1.0
.8
.6
.4
.20
100
200
300
400
500
600
WS
A
B
C
10
5
7.5
F_D VS. WS PLOTS
(A) L/K = 5.0
(B) L/K = 7.0
(C) L/K = 10.0
K = (.135)(.135) FT. BAR

Fig. V-9

TABLE V-1

Computed Values for WS, $\frac{V^2}{WS - F_D}$ and $\frac{C_m}{\sqrt{g}}$

Run	Slope	$\frac{L}{K}$	Q	y_1	y_c	L	C_1	WS	$\frac{V^2}{WS - F_D}$	$\frac{C_m}{\sqrt{g}}$	C_{1m}
7	2.56	5	.97	.181	.195	.675	.656	62.3	.0381	.363	4.912
8	"	"	.93	.176	.190	"	.643	61.3	.037	.354	4.94
9	"	"	1.20	.212	.225	"	.741	69.0	.0437	.393	4.79
10	"	"	1.48	.244	.260	"	.839	76	.0503	.426	4.79
8	5.18	"	1.25	.172	.230	"	.611	122	.3343	.340	4.79
9	"	"	1.57	.210	.270	"	.685	139	.03725	.361	4.46
6	12.18	"	.80	.120	.170	"	.319	239	.09952	.181	3.53
7	"	"	.97	.130	.195	"	.362	244	.01378	.213	3.162
8	"	"	1.12	.140	.215	"	.408	260	.01543	.231	3.86
9	"	"	1.40	.165	.250	"	.457	280	.01947	.270	3.74
5	8.253	"	.97	.155	.195	"	.431	169	.0192	.252	4.28
6	"	"	1.17	.150	.220	"	.491	179	.0236	.282	4.407
7	"	"	1.33	.165	.240	"	.528	190	.0261	.300	4.33
8	"	"	1.71	.195	.280	"	.618	210	.0321	.335	4.32
9	"	"	2.33	.235	.350	"	.754	239	.0417	.388	4.44
7	11.335	7.5	1.46	.240	.255	1.013	.397	512	.00741	.201	2.26
8	"	"	1.74	.225	.285	"	.493	490	.0120	.252	2.95
9	"	"	2.00	.238	.315	"	.548	509	.0142	.277	3.122
10	"	"	2.37	.255	.355	"	.623	533	.0174	.308	3.36
11	"	"	2.32	.280	.350	"	.575	569	.01373	.277	2.87
12	3.085	"	1.90	.430	.300	"	.875	161	.0305	.414	4.77
13	"	"	2.06	.447	.325	"	.919	167	.0321	.426	4.19
14	"	"	2.34	.470	.350	"	.997	176	.0354	.453	4.29
9	5.89	"	1.76	.378	.290	"	.665	269	.0203	.331	3.705
10	"	"	1.92	.388	.305	"	.702	276	.0222	.349	3.81
11	"	"	2.2	.410	.335	"	.765	293	.0246	.370	3.87
11	4.132	10	2.72	.328	.385	1.35	1.016	313	.0276	.460	4.42
7	10.26	"	2.26	.395	.345	"	.616	644	.0128	.308	3.24
8	"	"	2.78	.275	.390	"	.733	659	.01754	.360	3.683
6	7.77	"	1.90	.287	.300	"	.561	658	.00771	.240	2.717
7	"	"	2.10	.270	.325	"	.643	512	.01316	.310	3.280
8	"	"	2.37	.284	.355	"	.703	530	.0152	.337	3.438
9	"	"	2.65	.300	.375	"	.761	552	.01693	.358	3.560
10	"	"	3.03	.320	.410	"	.836	579	.0192	.381	3.710

TABLE V-2

Computed Values for Drag Coefficient C_D
and Conventional Chézy Coefficient

Run	Slope	$\frac{L}{K}$	Q	y_1	V_1	$y_1 + K$	V	C_D	C_{D1}	C_n	C
7	2.46	5	.97	.181	2.68	.316	1.535	.472	.155	2.06	.471
8	"	"	.935	.176	2.66	.311	1.501	.482	.154	2.01	.458
9	"	"	1.200	.212	2.83	.347	1.730	.420	.158	2.23	.549
10	"	"	1.48	.244	3.03	.379	1.95	.376	.155	2.42	.639
8	5.18	"	1.25	.172	3.63	.307	2.03	.532	.166	1.93	.438
9	"	"	1.57	.210	3.74	.345	2.27	.488	.179	2.05	.506
6	12.18	"	.80	.120	3.33	.260	1.57	1.366	.292	1.03	.201
7	"	"	.97	.130	3.73	.265	1.83	1.090	.266	1.21	.240
8	"	"	1.120	.140	4.00	.280	2.00	.990	.248	1.31	.265
9	"	"	1.400	.165	4.24	.300	2.33	.827	.249	1.53	.321
5	8.253	"	.970	.135	3.49	.270	1.795	.840	.210	1.43	.288
6	"	"	1.17	.150	3.90	.285	2.050	.712	.197	1.60	.336
7	"	"	1.330	.165	4.03	.300	2.220	.659	.201	1.70	.373
8	"	"	1.710	.195	4.38	.330	2.590	.551	.192	1.90	.450
9	"	"	2.330	.235	4.96	.370	3.150	.449	.182	2.20	.570
7	11.335	7.5	1.46	.240	3.040	.375	1.945	1.803	.328	1.14	.302
8	"	"	1.74	.225	3.87	.360	2.42	1.271	.495	1.43	.371
9	"	"	2.00	.238	4.20	.373	2.680	1.130	.460	1.57	.415
10	"	"	2.37	.255	4.65	.390	3.040	.921	.395	1.75	.480
11	"	"	2.32	.280	4.14	.415	2.795	1.14	.516	1.57	.449
12	3.085	"	1.90	.430	3.22	.430	2.210	.608	.286	2.35	.688
13	"	"	2.06	.447	3.31	.447	2.310	.584	.284	2.42	.731
14	"	"	2.34	.470	3.49	.470	2.49	.540	.274	2.57	.801
9	5.89	"	1.76	.378	3.62	.383	2.33	.860	.395	1.88	.503
10	"	"	1.92	.388	3.79	.388	2.47	.799	.359	1.98	.539
11	"	"	2.20	.410	4.00	.410	2.68	.734	.330	2.10	.596
11	4.132	10	2.72	.328	4.146	.463	2.93	.700	.351	2.61	.812
7	10.26	"	2.26	.395	4.346	.395	2.86	1.394	.604	1.75	.475
8	"	"	2.78	.275	5.055	.410	3.39	1.103	.497	2.05	.571
6	7.77	"	1.90	.287	3.31	.422	2.25	1.620	.748	1.36	.440
7	"	"	2.10	.270	3.89	3.00	2.59	1.33	.587	1.76	.499
8	"	"	2.37	.284	4.17	3.10	2.83	1.195	.550	1.91	.552
9	"	"	2.65	.300	4.42	3.222	3.05	1.07	.510	2.03	.603
10	"	"	3.03	.320	4.73	3.37	3.330	.966	.478	2.16	.667

TABLE V-3

Computed Values for $\frac{y_1 + K}{K}$

Slope	Run	L/K	y_1	K	$y_1 + K$	$\frac{y_1 + K}{K}$	$\frac{Q_m}{\sqrt{g}}$
2.56	7	5	.181	.135	.316	2.341	.363
"	8	"	.176	"	.311	2.304	.354
"	9	"	.212	"	.347	2.570	.393
"	10	"	.244	"	.379	2.807	.426
5.18	8	"	.172	"	.307	2.274	.340
"	9	"	.210	"	.345	2.555	.361
12.18	6	"	.125	"	.260	1.926	.181
"	7	"	.130	"	.265	1.963	.213
"	8	"	.145	"	.280	2.074	.231
"	9	"	.165	"	.300	2.222	.270
8.253	5	"	.135	"	.270	2.00	.252
"	6	"	.150	"	.285	2.111	.282
"	7	"	.165	"	.300	2.22	.300
"	8	"	.195	"	.330	2.444	.335
"	9	"	.235	"	.370	2.741	.388
11.335	7	7.5	.240	"	.375	2.778	.201
"	8	"	.225	"	.360	2.667	.251
"	9	"	.238	"	.373	2.763	.277
"	10	"	.255	"	.390	2.889	.308
"	11	"	.280	"	.415	3.074	.277
3.085	12	"	.295	"	.430	3.185	.414
"	13	"	.312	"	.447	3.311	.426
"	14	"	.335	"	.470	3.481	.453
5.89	9	"	.248	"	.383	2.837	.331
"	10	"	.253	"	.388	2.874	.349
"	11	"	.275	"	.410	3.037	.370
4.132	11	10	.328	"	.463	3.429	.460
10.26	7	"	.260	"	.395	2.926	.308
"	8	"	.275	"	.410	3.037	.360
7.77	6	"	.287	"	.422	3.126	.240
"	7	"	.270	"	.405	3.000	.310
"	8	"	.284	"	.419	3.100	.337
"	9	"	.300	"	.435	3.222	.358
"	10	"	.320	"	.455	3.37	.381

TABLE V-4

Computed Values for Modified Chézy Coefficient and $\frac{y_1}{K}$

Slope	Run	L	$\frac{L}{K}$	$\sqrt{g}$	C	$\frac{C_m}{\sqrt{g}}$	C_D	y_1	y_1/K
2.56	7	.675	5	5.675	2.06	.363	.472	.181	1.341
"	8	"	"	"	2.01	.354	.484	.176	1.304
"	9	"	"	"	2.23	.393	.420	.212	1.570
"	10	"	"	"	2.42	.426	.376	.244	1.810
5.18	8	"	"	"	1.93	.340	.532	.172	1.274
"	9	"	"	"	2.05	.361	.488	.210	1.556
12.18	6	"	"	"	1.03	.181	1.366	.125	.926
"	7	"	"	"	1.21	.213	1.49	.130	.963
"	8	"	"	"	1.31	.231	.990	.145	1.074
"	9	"	"	"	1.53	.270	.827	.165	1.222
8.253	5	"	"	"	1.43	.252	.840	.135	1.00
"	6	"	"	"	1.60	.282	.712	.150	1.111
"	7	"	"	"	1.70	.300	.659	.165	1.222
"	8	"	"	"	1.90	.335	.551	.195	1.444
"	9	"	"	"	2.20	.388	.449	.235	1.741
11.335	7	1.013	7.5	"	1.14	.201	1.80	.240	1.778
"	8	"	"	"	1.43	.252	1.271	.225	1.667
"	9	"	"	"	1.57	.277	1.130	.238	1.763
"	10	"	"	"	1.75	.308	.921	.255	1.889
"	11	"	"	"	1.57	.277	1.14	.280	2.074
3.085	12	"	"	"	2.35	.414	.608	.295	2.185
"	13	"	"	"	2.42	.426	.584	.312	2.311
"	14	"	"	"	2.57	.453	.540	.335	2.981
5.89	9	"	"	"	1.88	.331	.860	.243	1.800
"	10	"	"	"	1.98	.349	.799	.253	1.874
"	11	"	"	"	2.10	.370	.734	.275	2.037
4.132	11	1.35	10	"	2.61	.460	.700	.328	2.430
10.26	7	"	"	"	1.75	.308	1.394	.360	2.667
"	8	"	"	"	2.04	.360	1.103	.275	2.037
7.77	6	"	"	"	1.36	.240	1.620	.287	2.126
"	7	1.35	10	"	1.76	.310	1.33	.270	2.00
"	8	"	"	"	1.91	.337	1.193	.284	2.104
"	9	"	"	"	2.03	.358	1.07	.300	2.222
"	10	"	"	"	2.16	.381	.966	.32	2.370

TABLE V-5

Computed Values for Modified and Conventional Chézy Coefficient

Run	Slope	$\frac{L}{K}$	y_1	y_c	C	C_m	C	C_{1m}	C_1
7	2.56	5	.181	.195	.970	2.06	.471	4.912	.6569
8	"	"	.176	.190	.935	2.01	.458	4.94	.6430
9	"	"	.212	.225	1.20	2.23	.549	4.79	.7410
10	"	"	.244	.260	1.48	2.42	.639	4.79	.8393
8	5.18	"	.172	.230	1.25	1.93	.438	4.79	.6111
9	"	"	.210	.270	1.57	2.05	.506	4.46	.685
6	12.18	"	.120	.170	.80	1.03	.201	3.53	.319
7	"	"	.130	.195	.97	1.21	.240	5.162	.362
8	"	"	.140	.215	1.12	1.31	.265	3.86	.408
9	"	"	.165	.250	1.40	1.53	.321	3.74	.457
5	8.253	"	.135	.195	.97	1.43	.288	4.28	.431
6	"	"	.150	.220	1.170	1.60	.336	4.407	.491
7	"	"	.165	.240	1.330	1.70	.373	4.33	.528
8	"	"	.195	.280	1.710	1.90	.450	4.32	.618
9	"	"	.235	.350	2.33	2.20	.570	4.44	.754
7	11.335	7.5	.240	.255	1.46	1.14	.302	2.26	.397
8	"	"	.225	.285	1.76	1.43	.371	2.95	.493
9	"	"	.238	.315	2.00	1.57	.415	3.122	.548
10	"	"	.255	.355	2.37	1.75	.480	3.36	.623
11	"	"	.280	.350	2.32	1.57	.449	2.87	.575
12	3.085	"	.430	.300	1.90	2.35	.688	4.77	.875
13	"	"	.447	.325	2.06	2.42	.731	4.19	.919
14	"	"	.470	.350	2.34	2.57	.801	4.29	.997
9	5.89	"	.378	.290	1.76	1.88	.503	3.705	.665
10	"	"	.388	.305	1.92	1.98	.539	3.81	.702
11	"	"	.410	.335	2.20	2.10	.596	3.87	.765
11	4.132	10	.328	.385	2.72	2.61	.812	4.42	1.016
7	10.26	"	.395	.345	2.26	1.75	.475	3.24	.616
8	"	"	.275	.390	2.78	2.05	.571	3.683	.733
6	7.77	"	.287	.300	1.90	1.36	.440	2.717	.561
7	"	"	.270	.325	2.10	1.76	.499	3.280	.643
8	"	"	.284	.355	2.37	1.91	.552	3.438	.703
9	"	"	.300	.375	2.65	2.03	.603	3.560	.761
10	"	"	.320	.410	3.03	2.16	.667	3.710	.836

VI. SUMMARY AND CONCLUSIONS

After rechecking the measured drag forces as obtained by Al-Khafaji, the prediction equations for computing drag forces on a two-dimensional roughness element in rapid and tranquil flow were derived using dimensional analysis.

For rapid flow and (K = .135 x .135) ft. bars, the prediction equation is found to be:

$$F_D = 0.0169\ (S)^{.76}\ \left(\frac{L}{K}\right)^{1.13}\left(\frac{y_c}{K}\right)^{.86}$$

For tranquil flow and (K = .135 x .135) ft. bars, the prediction equation is found to be:

$$F_D = 0.0167\ (S)^{.665}\ \left(\frac{L}{K}\right)^{1.57}\left(\frac{y_c}{K}\right)^{.615}$$

and that for the (K = .3 x .3) ft. bars is found to be:

$$F_D = .316\ (S)^{.495}\ \left(\frac{L}{K}\right)^{.73}\ \left(\frac{y_c}{K}\right)^{1.02}$$

Using these equations, the drag forces F_D were computed and compared with those measured F_D. The following results were obtained:

1. For rapid flow and (K = .135 x .135) ft. bars, the percent deviations are as shown in Table IV-1.
2. For tranquil flow and (K = .135 x .135) ft. bars, the percent deviations are as shown in Table IV-2.
3. For tranquil flow and (K = .3 x .3) ft. bars, the percent deviations are as shown in Table IV-3.

As far as the relationships of Chézy and drag coefficients with other variables, the following findings were obtained:

1. Modified Chézy coefficient increases with L/K.
2. Modified Chézy coefficient increases with y_1.
3. C_D increases with L/K.
4. For constant L/K, C_D is found to decrease when C_m increases.
5. For constant L/K, C_D is found to decrease with increasing values of C.
6. For constant values of L/K, C_1 is found to decrease with increasing values of C_{1D}.
7. F_D is found to increase with increasing values of WS for constant L/K.

ACKNOWLEDGMENT

This thesis was written under the able and competent guidance of This particular study was based upon the extensive research work of at

The author wishes to express his appreciation to He also wishes to express his deep appreciation to for his ever present encouragement and guidance not only during the performance of this study but every time it is needed.

He wishes to thank every one of his teachers and classmates for their patient cooperation.

The author is also thankful to who helped type this thesis.

VIII. GLOSSARY

A Area of cross-section of flume

C_D Drag coefficient

C_m Modified Chézy coefficient

C Chézy coefficient

C_1 Modified Chézy coefficient at the crest

C_{1D} Drag coefficient at the crest

F_D Computed drag force

g Acceleration of gravity

K Characteristic height of roughness element

L Relative spacing between roughness elements

P Wetted perimeter

Q Discharge in ft^3

S Slope of the channel bed

V Mean velocity in ft./sec.

y_1 Depth of flow in feet

y_c Critical depth of flow in feet

W Weight of water between two consecutive roughness elements

γ Specific weight of water in lb./ft^3

ρ Density of water in slags/ft^3

$\bar{K}$ Conveyance factor

IX. BIBLIOGRAPHY

1. Al-Khafaji, A. N., "The Dynamics of Two-Dimensional Flow in Steep, Rough Open Channel," Ph.D. Dissertation, Utah State University, Logan, Utah, 132 p., 1961.

2. Brahm, A., "Element of Dams and Hydraulic Engineering," 1754 and 1757, Vol. 1, p. 105.

3. Chèzy Formula "Origin of the Chèzy Formula", Journal of Association of Engineering Societies, 18, 363-368, June, 1897.

4. Fan Chia Hwa, "A Study of Stable Channel Cross-Section in Hydraulic Engineering."

5. DuBois, P., "The Rhone and Stream with Movable Bed," Annals des Poches et Chassies, Ser. 5, Vol. 18, pp. 141-149, 1879.

6. Forchheimer, Philip, "Hydraulics", Teubner verlagsgesellschaft, Leipzig and Berlin, First Edition, 1924, p. 495, Third Edition, 1930, p. 551.

7. Ganguillet, E. and Kutter, W. R., "A General Formula for Uniform Flow of Water in Rivers and Other Channels", New York, John Wiley and Sons, 1889, 240 p.

8. Leighley, J. B., University of California Publication in Geography, Vol. 6, No. 1, pp. 1 - 22, 1923.

9. Lane, Emory, "Design of Stable Channels", Transaction American Society of Civil Engineers, Vol. 120, pp. 1234 - 1266, 1955.

10. Morris, H. M. Jr., "Flow in Rough Conduits", Transaction American Society of Civil Engineers, pp. 120, 373-410, 1955.

11. Mohanty, P. K., "The Dynamics of Turbulent Flow in Steep Rough Open Channels", Doctoral Dissertation, Utah State University, Logan, Utah, June 1959.

12. Olesen, O. J. and Q. L. Florey (Compilers), Bureau of Reclamation, Laboratory Report No. 2, Sp. 35, August 5, 1952.

13. Robertson, J. M. and H. Rouse, "On the Four Regimes of Open Channel Flow," Civil Engineering, 11-169-171, 1952.

14. Shih, Kwen, "Effect of Roughness on Flow Resistance and Froude Number for Tranquil Flow in Steep, Rough Channels," M.S. Thesis, Virginia Polytechnic Institute, 1962.

15. Sabir, Ramzan A., "Effects of Two-Dimensional Roughness Elements on Froude Number and Resistance Coefficients in Rapid Flow in Steep, Rough Rectangular Flume," M. S. Thesis, Virginia Polytechnic Institute, 1962.

16. Prandl, L., Uber Flussigkeitsbewegung bei sehr Kleiner Reibung, Verhandl. III International Math., Krongr., Heidelberg, 1904.

The vita has been removed from the scanned document

Abstract

EVALUATION OF DRAG FORCES IN STEEP, ROUGH FLUMES

This thesis is based on the analysis of data collected by Al-Khafaji at the hydraulics laboratory of Utah State University. The study consists of the evaluation of drag forces in terms of measurable quantities. Using dimensional analysis and the available data, equations for drag forces were developed in two flow regimes; namely, tranquil and rapid regimes.

Qualitative relationships between the Chézy C and the drag coefficient, C_D, were also developed as well as the behavior of both C and C_D with different pertinent flow and geometric variables.